MSc Thesis, Delft University of Technology, Faculty of Civil Engineering and Geosciences, Coastal Engineering section

ASMITA modelling of the Wadden Sea with focus on the Groningerwad

Assessing how the Groningerwad will respond to accelerated sea level rise

Thomas Albers 4687817
3-11-2023

Committee:
Prof. dr. ir. Z.B. Wang
Prof. dr. P.M.J. Herman
Dr. Y. Huismans
Drs. Q.J. Lodder

Acknowledgement

It has been a great honour to have been able to complete my master thesis working at both Rijkswaterstaat and Deltares. I would therefore very much like to thank my supervising committee for this opportunity, and also for all the guidance they have provided which has been extremely helpful and absolutely necessary. I would not have been able to complete this thesis without their help as well as the help of numerous other people. Especially I would like to thank Edwin Elias for making his bathymetrical maps of the Groningerwad available to me. The AMO department of Deltares and the Rijkswaterstaat department of Water, Verkeer en Leefomgeving for their help, and allowing me to attend their meetings and learn about what they do. The GGZ Delfland for their help in keeping myself organised enough to complete my studies. My close friends for making studying together enjoyable. And my father for his wisdom, and willingness to check the grammar of my work.

Thomas Albers

Oktober 2023

Summary

As part of the coastal maintenance program the Dutch coastline is repeatedly nourished. These nourishments are used to maintain and protect the Dutch coastline. One of the factors which determines the required nourishment volume is the erosion from the coastal profile. Currently some of the sediment eroded from the coastal profile adjacent to the Wadden Sea is transported into the Wadden Sea. The Wadden Sea is a sink for sediment. Consequently, the maintenance of this part of the Dutch coast is influenced by the development of the Wadden Sea. This is one of the reasons that the development of the Wadden Sea is the subject of extensive research.

One of the models used to study the development of the Wadden Sea is the ASMITA model. This model is aggregated in space and time to allow the development of a tidal basin to be predicted by empirical equilibrium relations. These empirical equilibrium relations rely on the following principle describing a tidal basin experiencing sea level rise. As the sea level rises the depth of a tidal basin increases. The tidal prism, i.e. the volume of water which enters, or leaves, a tidal basin then also increases. This increase in tidal prism causes an increase in the available sediment transport capacity. Which causes an increase in sediment transport. When this sediment settles the depth of the basin decreases. Consequently, decreasing the tidal prism and sediment transport (capacity). This process continues until a new equilibrium is reached. In which the volume of sediment transport matches the sea level rise rate.

For most basins of the Wadden Sea the ASMITA model has been used to make predictions of their future development for different sea level rise scenarios. However, for the Groningerwad, the part of the Wadden Sea between Schiermonnikoog and the Ems estuary, this is not the case. Because the eastern Wadden islands are not systematically nourished the sediment import into the Groningerwad does not influence current coastal maintenance programs. However, as sea level starts to rise it is possible that also this part of the Dutch coast requires systematic nourishment. Also not only does sediment move into and out of the Wadden Sea through the tidal inlets. Sediment is also moved eastward across the tidal divides within the Wadden Sea itself. A part of this eastward sediment flux ultimately ends up in the Groningerwad. It is for these two reasons that in this study the response of the Groningerwad to acceleration in sea level rise is studied.

The Groningerwad consists of five major basins, from west to east, the Eilanderbalg, Lauwers, Schild Sparregat and Ra. In order to predict how these five basins will respond to accelerating sea level rise their past and current developments form an important basis that needs to be understood. A review of existing literature studying the Groningerwad paints a picture of a dynamic area containing highly migratory channels. With the west of the Groningerwad, the Eilanderbalg and the Lauwers basins, showing the largest changes. Besides considering available literature, this study also used available bathymetry from the vaklodingen dataset from Rijkswaterstaat to determine the volumes of the different elements of a tidal basin which are required for the ASMITA model. This study of the bathymetry determined these volumes but also considered the more general development of the area. Finding similar results to those of the other studies of the Groningerwad that the Groningerwad is a dynamic area. And that the overall area of the Groningerwad has decreased in the last 30 years.

ASMITA models have been set up for each of the basins of the Groningerwad. For each basin the α parameters, the fitting parameters for the empirical equilibrium relations, have been fitted such that with 2 mm/a sea level rise the basin is in dynamic equilibrium. The horizontal exchange coefficients between the different elements in each basin have been determined based on the bathymetry and their underlying formulas. The sea level rise scenarios considered are based on the IPCC projections outlined in their fifth assessment report. Which have been translated to sea level rise scenarios for the Dutch coast by Vermeersen et al. (2018).

The results of the ASMITA modelling showed that the Ra basin responds fastest to the accelerating sea level rise. The Ra basin is followed by the Schild and Sparregat, which respond almost similarly to each other, and the Eilanderbalg and the Lauwers. Of which the Lauwers is the basin that responds slowest to the acceleration of sea level rise.

Based on the results of the ASMITA modelling and the information from the morphological study the following predictions are made regarding the development of the Groningerwad. The morphological study showed that the area of the Groningerwad is decreasing over time. The ASMITA model results also show that for rising sea levels intertidal volume is lost. Therefore, it is predicted that the islands Rottumerplaat and Rottumeroog will move more landward. Schiermonnikoog, the island west of the Groningerwad, has in the past moved eastward behaviour which is expected to continue. As the ASMITA modelling showed the Ra basin responds fastest and the Lauwers the slowest. Consequently, it is predicted that the Ra basin will gain area at the expense of the surrounding basins, Sparregat and Lauwers. The Lauwers basin which showed the slowest response to accelerating sea level rise, is predicted to lose area to the Schild and Eilanderbalg basin.

When comparing the results of the Groningerwad with other ASMITA models of the Wadden Sea this shows that the Groningerwad responds much slower and has a considerably smaller critical sea level rise rate than other Wadden Sea basins. Due to a lack of available data over a long enough time period the horizontal exchange parameters have not been fitted to available data. Because of this and the comparison of the results with other basins of the Wadden Sea it is assumed that in reality the Groningerwad will respond faster to accelerating sea level rise than predicted in this study. It is recommended to revisit this study when more bathymetric data is available, and it is possible to fit the horizontal exchange coefficients and α parameters to measured changes in the bathymetry.

Table of contents

Chapter 1 – Introduction

In order to maintain the Dutch coastline, the Dutch coast is structurally nourished with sediment according to the program: 'uitvoeringsprogramma kustlijnzorg'. In the 'Deltaprogramma 2022' (Ministerie van infrastructuur en waterstaat, 2021) it is stated that this method of maintaining the coastline is a proven method of maintaining the coastline. It is relatively cheap and allows the coastline to grow with sea level rise in a way that also provides value to nature and possibilities for recreation. The 'uitvoeringsprogramma kustlijnzorg' is based on the principle 'zacht waar kan, hard waar moet' (Deltaprogramma Kust, 2014, p. 22). This should be interpreted as where a soft solution is possible it will be applied. But if a soft solution is unfeasible, for instance due to space limitations or economic unfeasibility, a more hard solution is chosen.

Nourishment is a proven soft strategy to maintain the present coastline. Its feasibility is, partly, determined by the volume of sediment that needs to be nourished per unit of time. This nourishment volume is determined by the amount of sediment which erodes from the coastal profile together with the beach area 'lost' or 'set back' due to sea level rise. Currently the Wadden Sea is a sediment sink for the adjacent coastal beaches (Stive, 1990). Because of this the development of the Wadden Sea has an effect on the amount of sediment which erodes from the coastline around the Wadden Sea. This, in turn, has an effect on the required nourishment volumes. In order to make a decision on the feasibility of nourishments on the Wadden Sea island beaches and adjacent North Holland coastline, insight in the magnitude of sediment import into the Wadden Sea is of importance. This is one of the reasons that the development of the Wadden Sea has been subject of extensive study (Stive, 1990; Elias et al., 2012; Wang et al., 2018; Elias, 2019; Wang & Lodder, 2019; Huismans et al., 2022).

One of the models applied to perform such studies of sediment import in the Wadden Sea is the ASMITA model. Due to its level of aggregation and by relating the development of tidal basins to empirical equilibrium relations the ASMITA model is able to assess the sediment transport in a tidal basin over a considerable time period. In studies by, amongst others, Huismans et al. (2022) and Wang & Lodder (2019) the ASMITA model was applied to make predictions of the six major basins within the Dutch Wadden Sea.

It is the goal of this thesis to improve the knowledge on the development of the Wadden Sea by applying the ASMITA model to the basins of the Groningerwad, a part of the Wadden Sea which has not yet been modelled with ASMITA. Currently, erosion of the islands adjacent to the Groningerwad does not yet warrant intensive nourishment. However, as sea level rises, the influence of the development of this part of the Wadden Sea on their adjacent coast becomes more important. Which is why also studying the development of this part of the Groningerwad is of interest. This introductory chapter continues with outlining sediment transport patterns within the Wadden Sea, presents the main research question considered in this thesis and ends with the methodology that is applied to answer the research questions.

1.1 Sediment transport within the Wadden Sea

The net sediment transport in and out of the Wadden Sea, or in and out of tidal basins in general, is governed by a large number of different processes. Among these are for instance transport due to residual flow or due to tidal asymmetry (Wang et al., 2018). These processes and mechanisms govern large-scale sediment movement both into and out of the basin. The net sediment transport, however, depends on subtle difference within these processes, which are sometimes difficult to determine. Because of this difficulty empirical relations have been made which match observations of the development of intertidal basins to certain parameters for which it has been observed that there is some kind of relation. These empirical relations can thus be used to describe the development of tidal basins over long time periods. These equilibrium relations rely on tidal basins having an equilibrium state.

Eysink (1991) has summarized a number of these empirical relations relating basin development to basin geometry and the tidal prism. These relations follow the following principle, as sea level rises the depth of the basin becomes larger. As the depth of the basin becomes larger the tidal prism, which is the amount of water entering/leaving the tidal basin per flood/ebb cycle, and the cross-sectional area of flow also increase. A graphical representation of the increase of tidal prism and cross-sectional area is given in the middle image in figure 1. Because of these increases in the tidal prism and the cross-sectional area an increase in basin depth also increases the sediment transport into the basin. When the conditions are such that this additional sediment, which is transported into the basin, is allowed to settle, it increases the bed level. Which decreases the depth and, by extension, the tidal prism and the cross-sectional area of the basin as can be seen in the bottom image of figure 1. This decrease in depth, in turn, decreases the sediment transport capacity. This interaction empirically describes how a tidal basin grows with sea level rise. It relies on there being an equilibrium state between sediment transport and sea level rise. It is the basis for the equilibrium relations that have been derived for tidal basins, as summarized by Eysink (1991) and these are further considered in chapter 3.

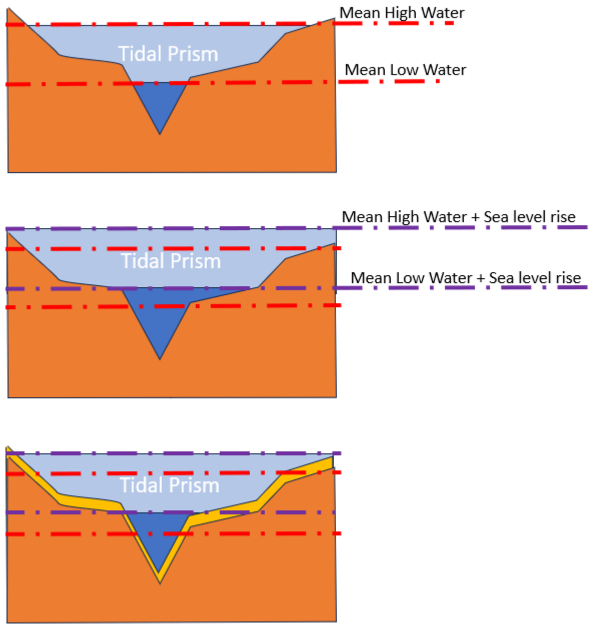

Figure 1 Empirical description of the development of a tidal basin experiencing sea level rise.

Even though tidal basins can keep up with sea level rise, this effect is not indefinite. As sea level rise rates accelerate a new balance forms between sea level rise and sediment import into the basin. A larger sea level rise rate requires a larger sediment import which requires a larger basin depth. Consequently, as sea level rise rate accelerates the new corresponding equilibrium state requires a deeper basin meaning a loss of intertidal area. At a certain point, the rate of sea level rise becomes so fast that all intertidal area is lost. This occurs when no new equilibrium between sea level rise and sediment import can be established.

Besides net sediment import caused by sea level rise, another reason for sediment import into the Wadden sea is the effect of closure works that have been performed in the last century. Due to these closure works the equilibrium of (parts of) the Wadden Sea has been disturbed. This resulted in a lot of sediment import (Elias et al., 2012). The Groningerwad area, which is the area of interest in this study, has not been directly influenced by closure works in the past. Nonetheless, in the general picture of the development of the Wadden area, the effects of the closure works are not to be overlooked.

In the Wadden sea the largest sediment fluxes, the net sediment movement, occur across the tidal inlets. Through these inlets sediment is imported or exported to maintain, or reach, an equilibrium. If net transport occurs the equilibrium is disturbed, either due to accelerating sea level rise and/or closure works. The tidal inlets however are not the only places where, net, sediment transport occurs. A study of water flow within the Western Wadden Sea basin for different forcing conditions, such as tide, waves and wind, has been performed by Van de Waal (2007). This study concluded that for these different forcing conditions there is always some flow across the tidal divides, the ‘border’ between two basins. Although this flow is rarely of considerable magnitude there are conditions where the flow and resulting sediment transport across the tidal divides cannot be disregarded. This is also shown by Elias et al., (2012) who showed that without, net, sediment transport across the tidal divides the observed developments of the sediment volumes within the Wadden Sea could not occur. Also, the study of Van Weerdenburg (2019) shows that the wind has a major effect on transport across the tidal divides, especially for storm conditions which is not surprising considering the energy contained in storm events.

Elias (2019) reports on the sediment balance in the Wadden Sea and considers and combines the different processes which determine sediment movement in, out and through the Wadden Sea. These findings are presented in figure 2. The net sediment transport into the basins through the inlets, which is caused by rising sea levels or deviation from the equilibrium state due to closure works, contains the largest sediment fluxes within the Wadden Sea, as denoted by blue arrows in figure 2. Cross basin transport, represented by the orange arrows in figure 2, is small but not negligible and this study has shown that some sediment is transported to the Groningerwad which lies east of the in figure 2 shown map of the Wadden Sea. This report on the sediment balance of the Wadden Sea was made by considering detailed trend analysis for current and long-term morphological development. It concludes that, in the long-term, in all the basins in figure 2 combined, a net sedimentation of 9.0 Mm^3/year occurs. And that again, in the long-term all the coastal profiles considered in figure 2 show erosion with a net value of about 9.3 Mm^3/year. These findings corroborate the fact that the Wadden Sea is a sediment sink for the adjacent coasts.

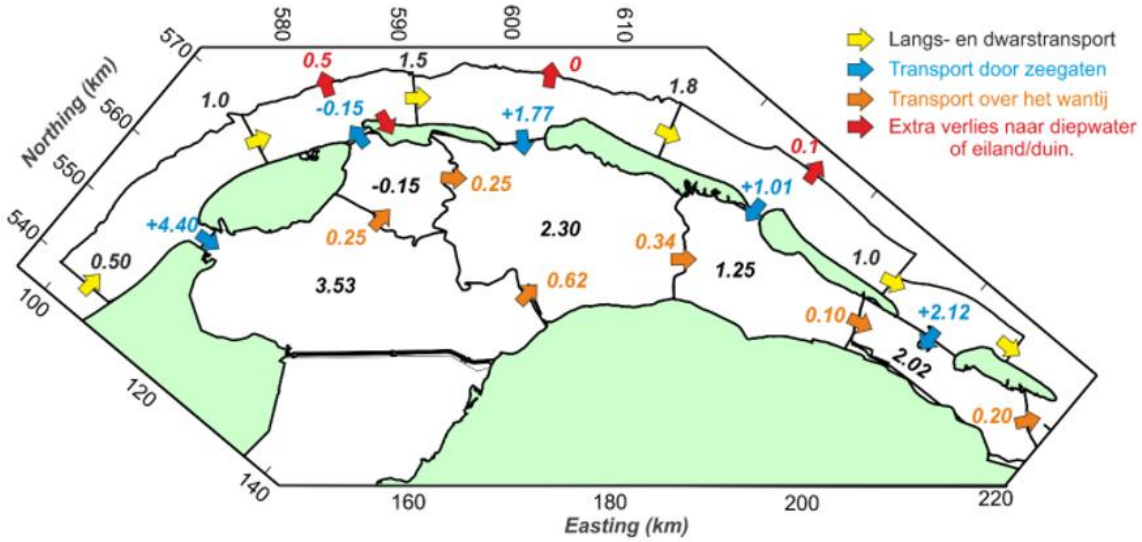

Figure 2 Sediment transport patterns in the Wadden sea from Elias 2019 p75 image d. In this image the yellow arrows refer to along and cross shore transport. The blue arrows refer to the transport through the tidal inlets. The orange arrows the cross-basin transport and the red arrows the loss to deeper water or the islands.

The study by Huismans et al. (2022) considers the six basins of the Wadden Sea shown in figure 3. The Groningerwad, which consists of a number of smaller basins that lie between the Zoutkamperlaag and Ems Estuary (to the right in figure 3), was not included in their study. For the Eastern Wadden Sea islands it has not yet been necessary to maintain their coastlines with a systematic nourishment strategy. Therefore, from a nourishment and or coastline maintenance perspective, the sediment import to the basins of the Groningerwad currently is not of that much importance. However, as the sea level rise rate increases, it may well be that in the future the coastal profile of the eastern Wadden Sea islands requires more maintenance. Also, as shown in the 2019 study by Elias (see figure 2), sediment moves eastward through the Wadden Sea and ends up in, or passing through, the Groningerwad. Further understanding of the to be expected development of the Groningerwad will also improve the understanding of these processes, which in turn reflects back on coastal maintenance strategies. It is for these reasons that the Groningerwad is chosen to be the study area of this thesis.

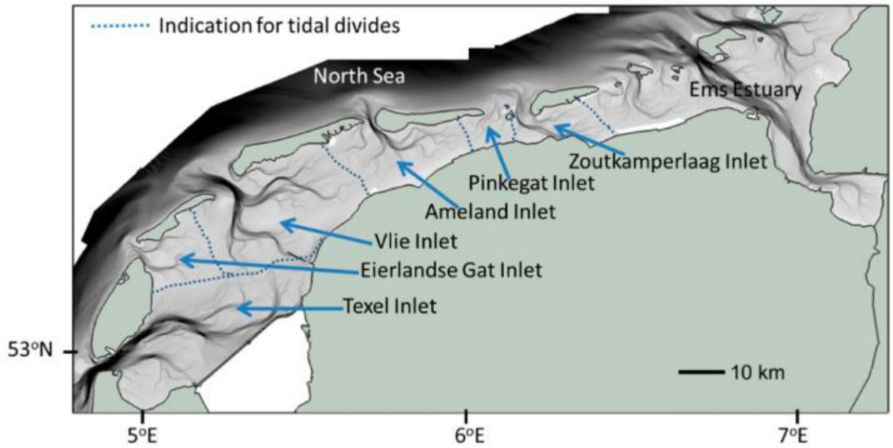

Figure 3 The tidal basins of the Wadden Sea for which in Huismans et al. 2022 study ASMITA models were set up. Image after Lodder et al. 2019.

1.2 Research questions

The development of the Groningerwad area is of interest to the general development of the Wadden Sea, which in turn is of interest to the nourishment and coastline protection strategies of the adjacent coasts. It is the goal of this study to gain insight in the development of the Groningerwad and how it will be affected by different sea level rise scenarios. Therefore, the main research question of the thesis is formulated as follows: '*How does the Groningerwad area respond to sea level rise*?

To answer this research question two main sub-questions have been determined. The first focuses on the current morphological developments within the Groningerwad. The second focuses on predictions of future developments within the Groningerwad. An additional third sub-question considers the effect of cross basin sediment transport on basin development. The exact formulation of the sub-questions is as follows:

The first sub-question is: '*What are the past and current morphological developments in the Groningerwad area?*' To understand and predict how the Groningerwad area will respond to sea level rise it is beneficial, if not crucial, to understand what the past looked like and what current developments are.

The second sub-question is aimed at predicting the response of the Groningerwad to sea level rise: '*What is the projected response of the Groningerwad area for to increasing sea level rise rates?*' This question is closely related to the main research question. By considering the development of the Groningerwad as predicted by a model it aims to give insight into the development of the Groningerwad area under sea level rise, which is the main goal of this thesis.

The third, or additional, sub-question is: '*How does the inclusion of inter basin morphological reaction due to residual flow across the Groningerwad area affect the response to sea level rise?*' Basin development is dominated by the net sediment transport through the inlet, but tidal inlets are not the only place where net sediment transport occurs. This sub-question considers the additional effect of cross basin transport to determine its relevancy in the development of the Groningerwad. Given that this would also hold for cross basin transport between tidal basins in a more general sense. This sub-question also considers interaction between tidal basins in a more general sense, which is why this third sub-question is considered an additional sub question.

1.3 Methodology of the different sub-questions

1.3.1 Sub-question 1. morphological study

To determine the current and past development of the Groningerwad, and answer the first sub-question, a number of past reports and studies on the development of the Groningerwad and surrounding area are considered. Furthermore, analysing available bathymetrical data from the 'vaklodingen' database provides insight into the development of the Groningerwad. Specific attention is given to the parameters that are also produced by the ASMITA model which is the model that is used to answer the second sub-question. These parameters include the development of the sediment volume of the ebb tidal delta, the sediment volume of the intertidal flat area and the water volume of the channels. They form one of the main focusses of the first sub-question. Further attention is given to the general development of the Groningerwad, for instance, by producing hypsometric curves, which provide insight in the development of a tidal basin. In the study by Nederhoff in 2017 hypsometric curves were produced for the mayor inlets of the Wadden Sea. It is also the goal of the first sub-question to produce such curves for the inlets of the Groningerwad.

1.3.2 Sub-question 2 prediction of effect of sea level rise by ASMITA modelling of the Groningerwad

As already mentioned, the ASMITA model is selected to predict the response of the Groningerwad to accelerated sea level rise and answer the second sub-question. The ASMITA model is an aggregated model that predicts basin development for considerable time periods by considering the empirical relations to describe basin developments. Given that the effects of sea level rise measurably occur over long time periods, this model is chosen to make predictions on the effect of sea level rise on the Groningerwad. The ASMITA model schematizes a tidal basin into a number of morphological elements: the ebb tidal delta, the channels, and the intertidal area. These elements have already been mentioned in the previous section as the morphological study seeks to determine the volumes of these elements to provide starting values for the modelling campaign. The sea level rise scenario's that are considered are based on IPCC rates from the fifth assessment report which have been used by Vermeersen et al. (2018) to determine sea level rise scenarios for the Dutch coast. These sea level rise scenarios have also been used in the study of Wang and Lodder (2019).

1.3.3 Sub-question 3 effect of cross basin transport

As for the importance of cross basin transport, it has been found by Van Weerdenburg (2019) that in the Ameland basin there is a residual eastward directed sediment transport, which crosses the tidal divides behind Terschelling in the west and Ameland in the east. In this study it is also shown that the transport across both divides differs by about a factor 10. How this translates to the cross tidal divide transport in the Groningerwad is something that needs to be considered. Nonetheless, given that there is some sediment transport across tidal divides. And it has been shown that the sediment budget cannot be closed without cross tidal divide transport in other parts of the Wadden Sea (Elias et al., 2012). It is of interest to include, perhaps in the form of a sensitivity analysis, an investigation in the effect of the response to sea level rise when cross basin flow is included. In the study by Elias (2019) describing the sediment balance of the Wadden Sea the transport across the tidal divide between the Friesche zeegat and the Groningerwad, this is assumed to be some 0.20 million m^3 per year. This value provides a starting point when considering cross basin flow in the Groningerwad, and is used as the basis for an adapted ASMITA model in which this additional cross basin sediment flux is considered.

Chapter 2- Morphological study of the Groningerwad

In order to understand and be able to predict how the Groningerwad area will develop in the future insight into the past and current developments is necessary. This chapter focuses on these past and current morphological developments of the Groningerwad and is split into two main parts. Part one provides a literature review on the development of the Groningerwad. Part two comprises a study of bathymetrical data of the Groningerwad area. Besides gaining insight into the current developments of the Groningerwad the study of bathymetrical data also provides the starting values for the further ASMITA modelling, by determining element areas and volumes.

2.1 Studies of the Groningerwad

The Groningerwad is an area within the Dutch Wadden Sea positioned between the island Schiermonnikoog and the Ems estuary. As shown in the maps in figures 4 and 5 it consists of five basins from west to east: Eilanderbalg, Lauwers, Schild, Sparregat and Ra. Of these the Ra basin drains into the Ems estuary whereas the other four basins drain into the North Sea. Figure 4 shows a map with the geographical names of the islands, inlets channels and intertidal areas. Whereas figure 5 shows the area of the different tidal basins in 1990.

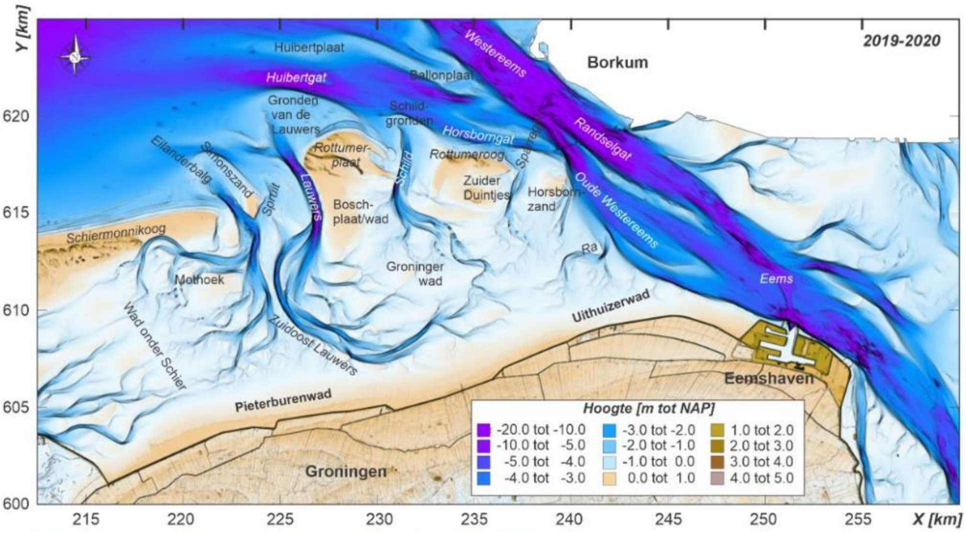

Figure 4 Map of the Groningerwad with geographical names of the major inlets, channels and intertidal areas, from Elias & Cleveringa 2021.

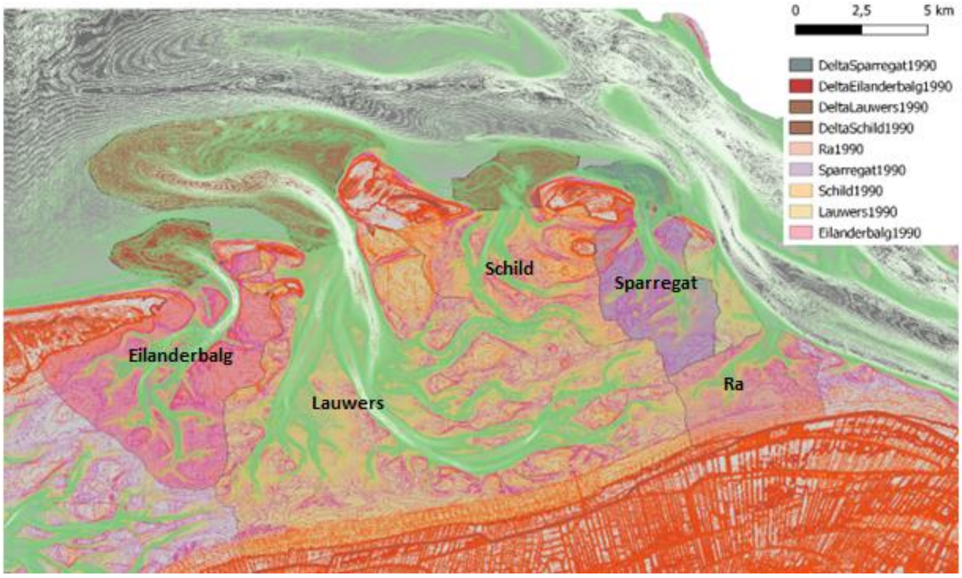

Figure 5 Map of the Groningerwad with the positions of the different basins based on the bathymetry in 1990.

In 2008 Cleveringa published an extensive report on the development of both the Ems Dollard and the Groningerwad. It found that the relatively small channels of the Groningerwad area have in time shown much larger variability than the larger channels surrounding the adjacent islands of Schiermonnikoog and Borkum. In the last 100 years or so the basin area of the Lauwers inlet has increased to the detriment of the basin area of the Schild inlet. And due to the eastward migration of the island Schiermonnikoog the Eilanderbalg channel also has moved eastward. Also, the eastward movement of the tidal divide of the Frisian inlet has affected the Eilanderbalg basin as a whole. Figure 6 shows the sedimentation and erosion rates in the Groningerwad and Eems Dollard area reported in the study by Cleveringa in 2008. Therein the middle area of the Groningerwad, areas 5 and 6 (i and h) to the left in figure 6, contains some highly migratory channels. The red areas in figure 6 show areas with sedimentation whereas the blue areas show areas of erosion. As the red areas of sedimentation are to the left of the channels and islands in the Groningerwad, it can be concluded that they tend to move eastward.

A study by Hoeksma et al. 2004 found that based on the vaklodingen the Eems-Dollard and Lauwers basins are eroding and the Eilanderbalg and Schild basins experience sedimentation. Lipari and Van Vledder (2008) find that, under storm conditions, a considerable amount of water is moved into the Ems Dollard basin from the Wadden Sea itself.

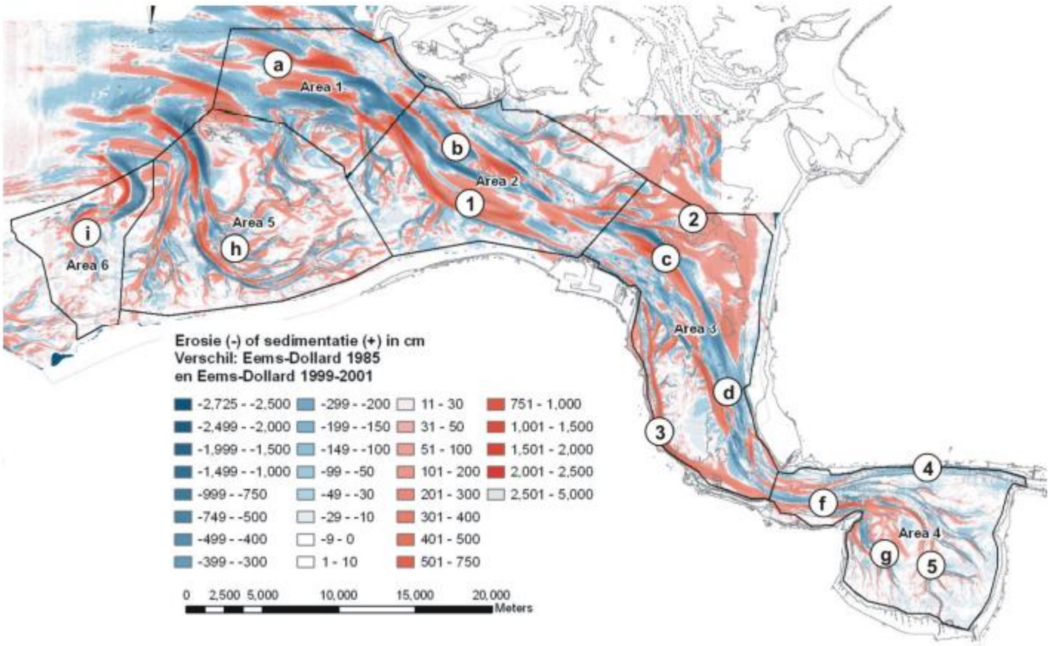

Figure 6: Erosion and sedimentation of the Ems Dollard and Groningerwad area. From Cleveringa, 2008 p22. Blue areas have shown erosion and red areas sedimentation. The Groningerwad lies to the east in the image contained in areas 5 and 6 (i and h)

The second study on the Groningerwad area considered was performed by Vermaas and Margues in 2017. They concluded that the largest changes in morphology can be found around the channels. The sedimentation and erosion induced by channel migration is considerably larger than the changes on the intertidal flats. The Schiermonnikoog island has expanded some 3.6 km towards the east in the period between 1990 and 2013. This expansion has reduced the size of the Eilanderbalg inlet, which despite the decrease in size has remained relatively constant in depth. Over the entire area of the Groningerwad considered in their study a volume increase of the intertidal flats of some $14.1 * 10^6 m^3$ was found. The largest increase was found along the beach strip of Schiermonnikoog, the Rottumerplaat and the intertidal area between the Spruit and the Lauwers in the southeast. Decreases in volume were found in the eastern intertidal area of the Uithuizerwad and between the Spruit and Eilanderbalg. The remaining areas show relatively small changes in volume which in general is increasing.

The third study on the Groningerwad considered was performed by Elias and Cleveringa in 2021, the 'kombergingsrapport' on the Lauwers and Groningerwad. This report concluded that the net changes in sediment volume in the Groningerwad over the study period from 1989 to 2019 were small. However, the gross changes, especially in the outer delta, have been considerable. The largest morphodynamical developments occurred in the Eilanderbalg and Lauwers basins. Here, due to the eastward development of Schiermonnikoog, the Eilanderbalg channel has also moved to the east absorbing the Spruit channel. The Spruit channel was formerly connected to the Lauwers channel and by absorbing this channel the Eilanderbalg basin has also gained a lot of area at the expense of the Lauwers basin. Further east the Schild basin has over the past period developed to a basin complete with channel system and ebb tidal delta. The Sparregat has over the past period remained the most stable showing the least morphological change.

Elias and Cleveringa (2021) showed similar results for the Groningerwad as Vermaas and Margues (2017), however, in a very detailed manner. They also considered the development of the islands Rottumerplaat and Rottumeroog. Since the introduction of the dynamic maintenance strategy by Rijkswaterstaat, large parts of the Dutch coastline have been maintained at a fixed position. These two islands however have been left to develop naturally which has allowed them to retreat landward. In doing so these islands show morphological behaviour which does not, generally, occur along the Dutch coastline anymore.

2.2 Analysis of bathymetrical data of the Groningerwad

The data used to perform this analysis are the vaklodingen of the Groningerwad area. These are maps of bathymetry collected by Rijkswaterstaat. Elias and Cleveringa (2021) used these vaklodingen to create maps of the bathymetry. These are also the maps of bathymetry that are used in this study. Table 1 shows a list of the bathymetrical maps and the years from which they have been constructed.

Table 1: List of bathymetrical maps and the time period from which they were obtained.

name	used years
GW1990	1989 – 1990
GW1997	1994 – 1997
GW2001	2000 – 2002
GW2007	2007 – 2008
GW2013	2012 – 2014
GW2019	2019 – 2020

One of the goals of this analysis is to determine the starting volumes of the different elements for the ASMITA modelling. Further explanation of the ASMITA model is presented in chapter three. However, a short summary of the element definitions within the ASMITA model is presented here as determining these volumes is one of the goals of the morphological study.

A three element ASMITA model schematizes a tidal basin into three elements: the outer delta, the channels of the basin and the intertidal flat of the basin. The volume of the outer delta is the excess sediment volume in reference to an uninterrupted reference beach profile. Figure 7 shows how the volumes of the two remaining elements the channel and intertidal area are defined. The volume of the channel is the water volume in the basin below the mean low water level. And the volume of the intertidal area is the sediment volume in between the mean low and high water levels.

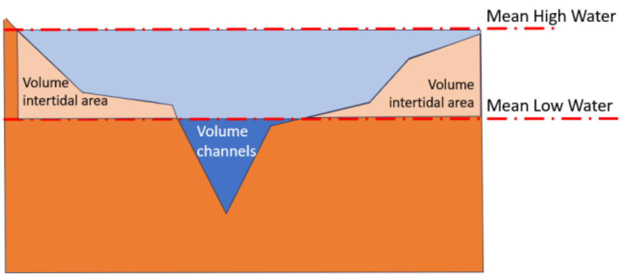

Figure 7 Schematic representation of the volume of the intertidal and channel element.

For the determination of these volumes the mean low and high water levels are needed. The water level measurements of different measurement stations surrounding the Groningerwad are presented in the report 'kenmerkende waarden kustwateren en grote rivieren' (Dillingh, 2013). Figure 8 shows that in the surrounding of the Groningerwad the following four measurement stations are present: Huibertgat, Schiermonnikoog, Lauwersoog and Eemshaven. The water level data concerning the period 1990 and 1981-1990 is taken from the 'Rijkswaterstaat, Rijksinstituut voor kust en zee tienjarigoverzicht 1981 - 1990' (Rijkswaterstaat, 1994). For the period 2001-2010 the data is found in appendix G of the 'Rijkswaterstaat report on the characteristic values' (Dillingh, 2013). The relevant information is also presented in table 2.

Figure 8 Positions of measurement stations around the Groningerwad from Dillingh 2013

Table 2: Measurements of water level and tidal range surrounding the Groningerwad, water levels are in reference to NAP.

Measurement Station	Average High tide 1990 [cm]	Average Low tide 1990 [cm]	Average High tide 2001-2010 [cm]	Average Low tide 2001-2010 [cm]	Average water level 1981-1990 [cm]	Average water level 2001-2010 [cm]
Huibertgat	98.5	-115.2	104	-114	-6	4
Schiermonnikoog	109.1	-117.8	105	-122	1	5
Lauwersoog	106.8	-121.4	106	-126	0	4
Eemshaven	124.0	-130.6	122	-140	1	3
Average	109.6	-121.3	109.3	-125	-1	4

It is possible to determine the element volumes of the channels and intertidal flats of a given basin. To do so the bathymetrical maps from the vaklodingen/datasets used by Elias and Cleveringa (2021) and the average levels of mean high water and mean low water (Rijkswaterstaat, 1994; Dillingh, 2013) were used. In order to determine these volumes for the 5 basins of the Groningerwad it is necessary to determine each basin's exact area. In this study a tidal basin is defined as the area which lies landward of the barrier islands and is below the mean high water line. The tidal divide, the border between basins, is, when considering an intertidal flat between two basins, defined as the line where the steep and mild slopes of that intertidal flat meet. The definition of a steep or mild slope of an intertidal flat is based on the density of contour lines. The slope with the most contour lines in the smallest area is the steep slope of the intertidal flat and vice versa. When considering two channels of different basins the tidal divide is defined as the line which crosses the shallowest part of these channels. The area of the ebb tidal delta lies seaward of the barrier islands and extends to include the deviation from the surrounding beach profile caused by the presence of the tidal inlet. Consequently, the border of the ebb tidal delta is defined as the border of the outer sills and banks surrounding the tidal inlet on the seaward side. With this definition of the area of a tidal basin and ebb tidal delta the following steps are followed to determine the basin area from the available bathymetry.

The boundaries of a tidal basin are found at:

1. The shortest path across the inlet;
2. the line of average highwater (1.09 m NAP, see table 2) between sea and (is)land;
3. the sills where channels from different inlets meet;
4. the sharp edges of the intertidal flats.

The boundaries of the ebb tidal delta:

1. The shortest path across the inlet;
2. along the edge of the beach profile of the surrounding islands;
3. through the largest concentration of elevation contour lines at the seaward edge.

Following this procedure, and definition of a tidal basin/ebb tidal delta, creates the following basin division for the Groningerwad for the bathymetrical map of 1990 which is shown in figure 9. Similar images have been created of the remaining bathymetrical maps showing the area of the different basins. These maps can be found in appendix A.

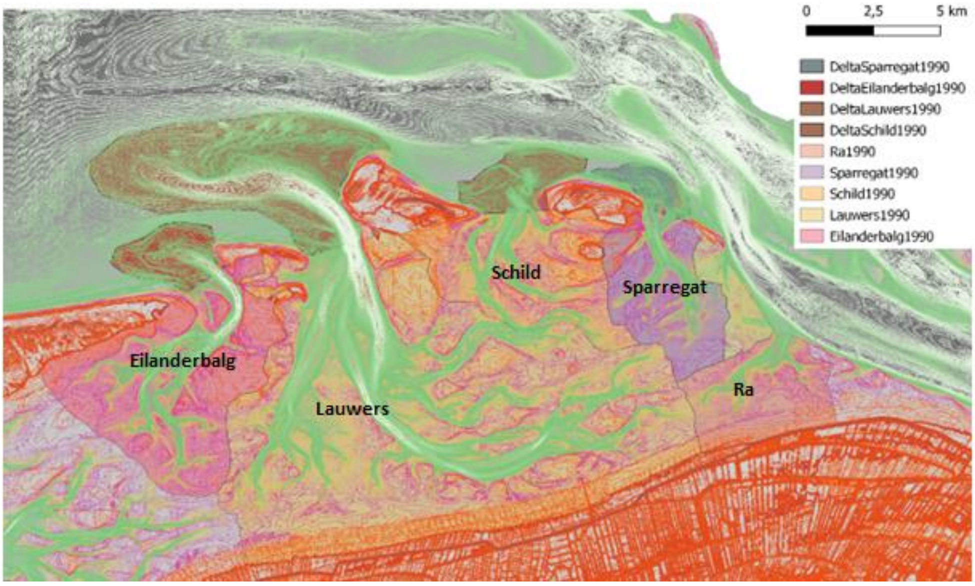

Figure 9 Map of the Groningerwad with the positions of the different basins based on the bathymetry in 1990.

By determining the boundaries of the basins and their ebb tidal deltas the areas of these elements can be determined. The area of the ebb tidal delta equals the area surrounded by its boundaries. The area of the channel and intertidal area follow from the area surrounded by the basin boundaries which is either below or above the average low water line respectively.

With the areas of the elements known, their volumes can also be determined. For the intertidal area this constitutes the sediment volume in between mean low and high water. For the channel it is the water volume below mean low water (see also figure 7). And for the ebb tidal delta the volume considered is the excess sediment volume caused by the inlet i.e., the difference in sediment volume between the inlet and an uninterrupted beach profile.

With the bathymetry and the mean high and low water levels known the volume of the channel and intertidal area can be directly determined. The volume of the ebb tidal delta however requires an uninterrupted beach profile with which the bathymetry can be compared. To create this uninterrupted beach profile the following formula is used:

$$d = 0.55 * x^{\frac{2}{3}}$$

Where d is the depth in meters and x the distance from the shore in meters. This formula and the value 0.55 which have been found for the beach profile of Ameland (Bosboom and Stive, 2021)

With this formula an uninterrupted beach profile can be created. In this study the created beach profile starts at zero and extends perpendicular to the entrance of the inlet. Subsequently subtracting the beach profile from the bathymetry within the area of the ebb tidal delta yields the ebb tidal delta volume. Figure 10 shows this process in three images, the top shows the reference beach profile. The middle image shows the bathymetry of the ebb tidal delta of the Sparregat. The bottom image shows the difference between the reference beach profile and bathymetry from which the volume of the ebb tidal delta can be calculated.

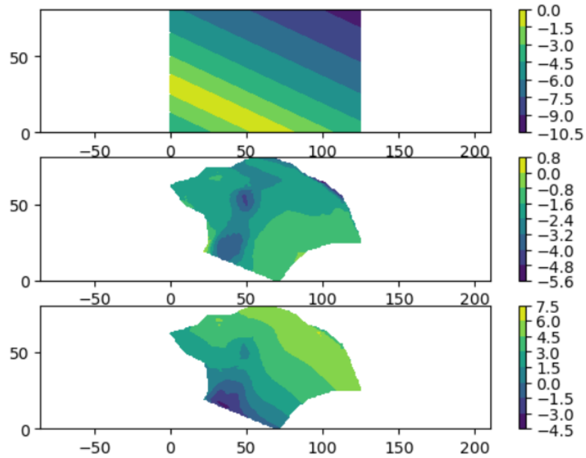

Figure 10 Determination of the ebb tidal delta volume, above the reference beach profile, middle the bathymetry of the ebb tidal delta of the Sparregat, below the difference between the two which determines the volume of the ebb tidal delta.

The average values of the area and volume of the different elements are presented in the table 3. Volume and area for each basin per bathymetrical map can be found in appendix B.

Table 3 Average area and volume of the basins of the Groningerwad

	Eilanderbalg	Lauwers	Schild	Sparregat	Ra
Intertidal					
Area [m^2]	37.464.200	89.517.000	27.014.267	14.861.667	15.642.533
Volume [m^3]	39.984.124	95.403.260	28.063.310	12.967.303	15.451.775
Channel					
Area [m^2]	9.036.200	33.844.600	5.375.267	2.882.067	1.809.267
Volume [m^3]	22.044.862	92.516.296	10.048.023	3.697.511	1.790.252
Delta					
Area [m^2]	11.391.600	41.006.800	6.922.267	3.233.000	n.a.
Volume [m^3]	48.907.965	279.146.295	24.058.325	9.706.049	n.a.

Note that for the Ra no delta area and volume have been determined. As the Ra drains into the Ems estuary, and not in the North Sea directly, applying the reference beach profile would not give realistic results. Also, it has been found difficult to determine a specific ebb tidal delta area within the Ems estuary.

Based on this information and definition it is concluded that the combined area of the Groningerwad basins over the time period from 1990 to 2019 has decreased from some 255 km^2 to 237 km^2 as shown in figure 11. This considers the area of the basins as defined in this study only. Within this definition the area of the saltmarshes and islands in the Groningerwad are not included.

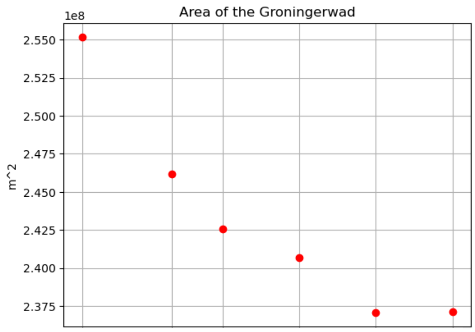

Figure 11 Area of the Groningerwad basins

The area and volume development of the respective basins are presented in figures 12 and 13 and show that the area of Eilanderbalg basin remains rather constant until in 2019 it gained a lot of area from the Lauwers basin due to a channel cross-over from the Lauwers to the Eilanderbalg. The Lauwers basin, over the study period, has decreased in size, including the channel cross-over in 2019. The Schild basin, on the other hand, over time increases in size. The areas of the Sparregat and Ra basins both remain rather constant. These findings are, overall, in line with what Elias and Cleveringa (2021) found. They determined that the largest changes occur in the Eilanderbalg and Lauwers basins. They also report that the Schild basin develops and the Sparregat remains rather constant. The volume of the outer delta of the different basins shows quite a large spread which makes it difficult to determine a distinct pattern.

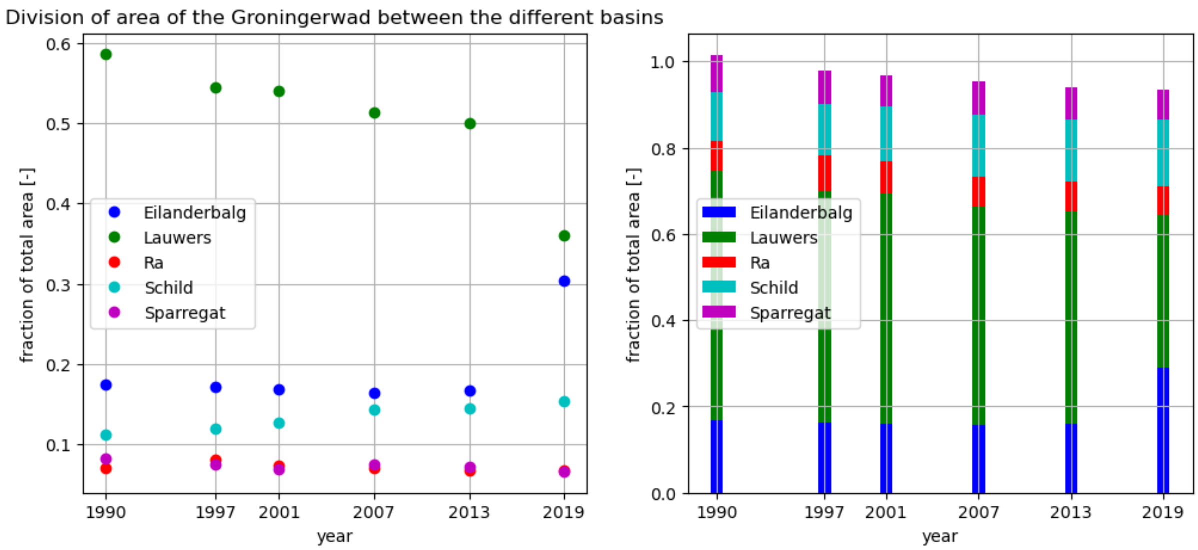

Figure 12 Division of area of the basins of the Groningerwad, note that the area is normalized to the average total area and that the total area has decreased over time (see also figure 11).

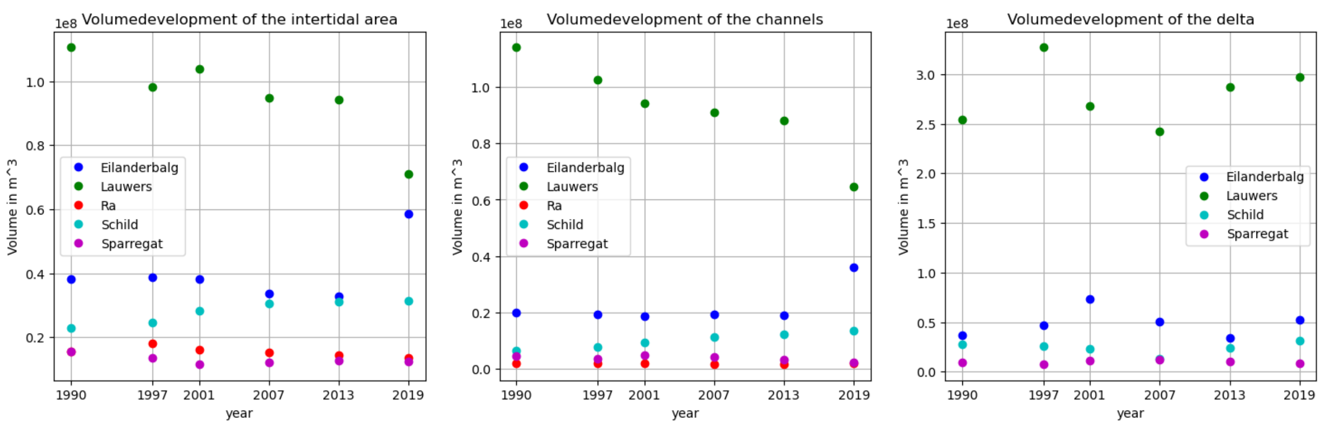

Figure 13 Division of volume of the different elements, left intertidal flat, middle channel, right delta.

2.2.1 Hypsometry

Hypsometric curves are often used to describe the relation between the bathymetry, the depth of the basin, and area. In this study hypsometric curves have been made for all five basins which are shown in figure 14 (and in appendix C). In both graphs in figure 14 the area is normalized to the maximum area of the different basins of the Groningerwad. The left graph shows the relation between area and the bathymetry in m with respect to NAP. The graph on the right shows the relation between the depth normalized to the depth at the 95 percentile of that basin and the normalized area. In the second graph the depth values above the 95 percentile of each basin, the deepest parts of each basin, are disregarded.

The first graph shows a tendency for the smaller basins to have steeper channels. The intertidal flat height is at about the same level for each basin. The larger basins however also have a larger channel area as they descend below the average mean low water line sooner than the smaller basins. This could however also be caused by the differences in area between the smaller and larger basins and the fact that the larger basins are also deeper. The second graph, which also is normalised in depth shows a much larger spread. This second graph gives an indication of which basins are closest to their equilibrium position. If a basin shows a larger spread, it is assumed to be further from equilibrium as explained in the next paragraph on basin stability. For both graphs it should be noted that the absolute area of the basins differ considerably, which is information that is filtered out due to the normalization process. Additionally, for the second graph given the normalization of the basin depth, all absolute volume information is also filtered out.

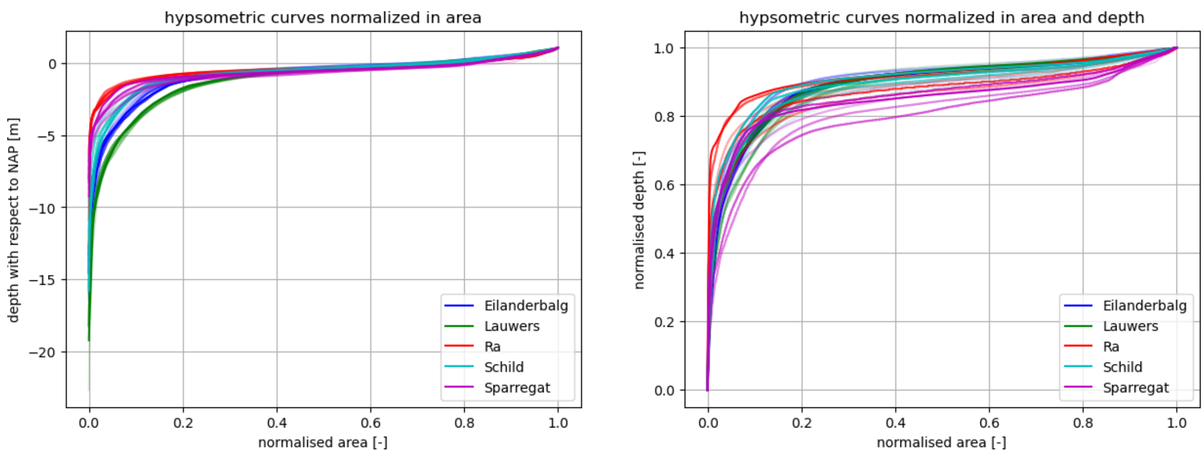

Figure 14 Hypsometric curves of the basins of the Groningerwad. Left, normalized to area. Right, normalized to both area and depth disregarding the values above the 95 percentile i.e., the deepest parts of the basins.

2.2.2 Basin stability

The information provided by the normalised hypsometric curves can be used to indicate which of the basins of the Groningerwad are closest to their morphological equilibrium. The assumption is made that, as a basin moves to its morphological equilibrium, not only its volume changes but also the distribution of said volume across the basin area. Figure 15 which is figure 10 of Huisman et al. (2022) shows how a tidal basin infills. As also mentioned in Huisman et al. (2022) a basin subject to accelerating sea level rise develops in reverse order. In the present situation, however, which is relevant for the determining which basin is closest to equilibrium, accelerating sea level rise is not relevant. The basin development as described by figure 15 shows that, as a basin develops, the distribution of volume also changes. Although, during the normalisation procedure, actual volume information is filtered out information on the distribution of said volume is retained.

Based on the normalised hypsometric graph it can be concluded that the Eilanderbalg and Lauwers basins are closest to equilibrium. The Sparregat and Ra are furthest from it whilst the Schild basin is somewhere in between these four. See also appendix C for graphs with the hypsometry plotted per basin.

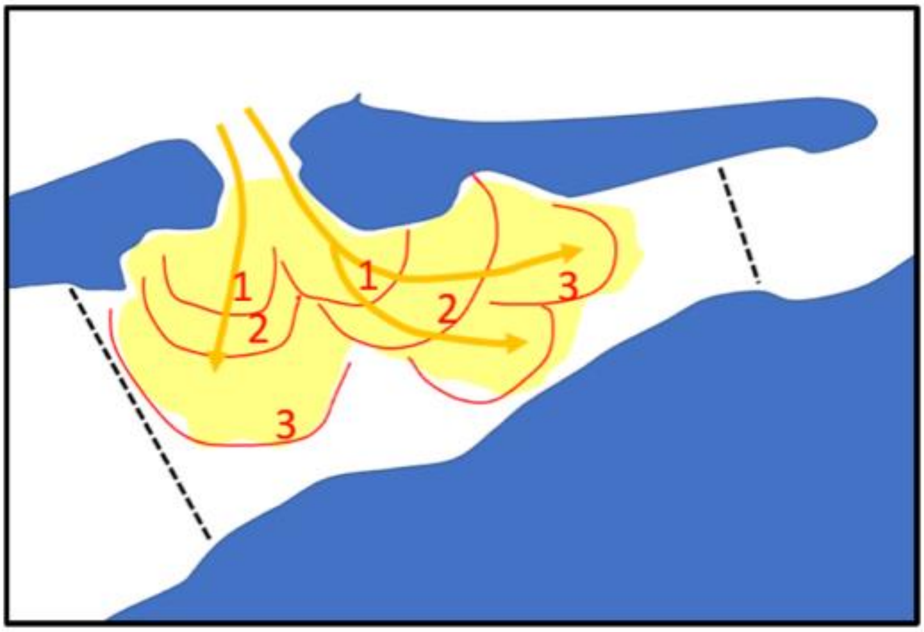

Figure 15 (Figure 10 of Huismans et al. 2022). Schematic of the development of the flood tidal delta. As the basin infills the flood tidal delta develops from stage 1 to 3 and beyond. If a sand deficit occurs the basin develops in reverse order. This image presented in Huismans et al (2022) is derived from (Westerhoff and Cleveringa, 1990; Van der Spek and Beets, 1992) their analysis of the development of the Wadden area.

2.3 Discussion and conclusion of the morphological study

Here we present the answer to the first sub-question that, as we recall, is: '*What are the past and current morphological developments in the Groningerwad area?*' The literature review sketched an image of a dynamic area with migratory channels. This finding was confirmed by the results of the study on the bathymetry. It shows for instance that the Eilanderbalg basin area was stable up to the period between 2013 and 2019 when it gained a lot of area at the expense of the Lauwers basin. According to the literature the islands in the Groningerwad (Rottumerplaat and Rottumeroog) have moved landward. This is corroborated by the study of bathymetry showing a decreasing area of the basins over time. An additional goal of the morphological study was to consider the volumes of the elements of a tidal basin as they are schematized by the ASMITA model. By considering the available bathymetry, and measurements of mean low and high water levels, these results have been found and presented in figure 13. Also, hypsometric curves of the different basins have been made, and are presented in figure 14, which show that the Eilanderbalg and Lauwers basins appear to be closer to their equilibrium position than Sparregat and Ra whilst the Schild basin situates somewhere in between.

Per basin the following conclusions can be drawn regarding their current developments:

2.3.1 Eilanderbalg

Based on the hypsometry the Eilanderbalg is the most stable of the basins of the Groningerwad. Due to the eastward expansion of the Schiermonnikoog island its inlet has also moved eastward. Over the study period it remains mostly constant in area except for the fact that, in the last bathymetry considered, a large area of the Lauwers became part of the Eilanderbalg because of a major channel cross-over between the two basins.

2.3.2 Lauwers

The Lauwers, based on the hypsometry, also appears to be one of the most stable basins. Considering its area however this shows that during the study period the Lauwers basin has become smaller, mostly due to the developing and growing Schild basin. But it also decreased in area due to a major channel cross-over between the Lauwers and Eilanderbalg as stated above.

2.3.3 Schild

The Schild basin has over the study period developed into a fully fletched basin. Compared to the other basins it is not as close to its morphological equilibrium as the Eilanderbalg and Lauwers, but closer than the Sparregat and Ra. Its area has showed a constant increase, mostly at the expanse of the Lauwers basin.

2.3.4 Sparregat

The Sparregat area has remained mostly constant over the study period. Based on the hypsometry it is together with the Ra furthest from its equilibrium position. This might by caused by the fact that the Sparregat and Ra both have the smallest areas, resulting in a larger sensitivity to changes in the bathymetry, as shown by the hypsometric curves.

2.3.5 Ra

The Ra has shown similar behaviour to that of the Sparregat remaining mostly constant in area over the study period. And together with the Sparregat the Ra is furthest from its equilibrium position for the same assumed reasons as mentioned above.

Chapter 3 ASMITA modelling of the Groningerwad basins

3.1 ASMITA model formulation

The ASMITA model is an aggregated model, for which the level of aggregation allows the use of empirical equilibrium relations to calculate morphological developments within a tidal basin. Townend et al. (2016) derives the mass balance equations used in ASMITA from the 3d convection diffusion equation. This was done to 'clarify the equivalence and differences between ASMITA and a process-based morphodynamic model (e.g. Delft 3D), and identify the physical nature of the (intertidal) dispersion.' (Townend et al., 2016, p489). The 3d convection diffusion equation is thus aggregated, both in space and time, until independent formulas for sediment transport and bed erosion can no longer be applied. Empirical relations can now be used to calculate the morphological equilibrium and morphological development. This means, however, that the ASMITA model is based on the same principles as a process-based model, be it, at a different level of aggregation. This different level of aggregation allows the ASMITA model to consider larger scales for longer time periods without becoming too computationally intensive. For this reason, the ASMITA model is selected to make predictions on the development of the Groningerwad under sea level rise.

The key concepts of the ASMITA model as described by Townend et al. (2016, p484) are as follows:

- 'Schematization into a number of geomorphologic elements;
- The state of each element is described by its volume and surface area, concerning either water or sediment;
- Integrated parameters of hydrodynamics i.e., the tidal prism and tidal range, are used;
- Empirical relationships define the morphological equilibrium for each element;
- Deviation from the morphological equilibrium causes a sediment demand or supply; and
- A gradient in sediment demand or supply drives sediment transport and by extension morphological change.'

The ASMITA model schematizes a tidal basin as a system containing three main elements as shown in figure 16. These elements are the intertidal flats, the channels of the basin and the ebb tidal delta. Where the ebb tidal delta also interacts with the outside world. These three elements each are characterized by a volume. In the case of the intertidal flat the characterizing volume is the sediment volume in between the mean low water level and the mean high water level. The characterizing volume of the channel element is the water volume in the basin below the mean low water level. And finally, the characterizing volume of the ebb tidal delta is the surplus volume of sediment which is present in the ebb tidal delta as opposed to the volume that would be there if there was no tidal inlet (See figures 7 and 10 in chapter 2.2 for a visual representation of the characterizing volumes of the different elements.).

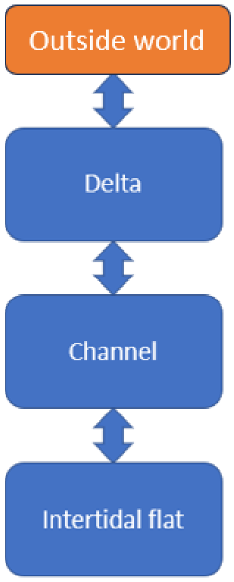

Figure 16 Order of elements within the ASMITA model

The ASMITA model relies on equilibrium relations that describe equilibrium volumes to the elements. These equilibrium relations for tidal inlets are derived from field measurements on the morphological development of a number of tidal basins (Eysink, 1991). The equilibrium relations are, in case of the channels and ebb tidal delta, related to the tidal prism. The equilibrium relations for the intertidal flat element are based on the basin area and tidal range. The exact formulation for the equilibrium volume of each element is as follows:

$$V_{ec} = \alpha_c * P^{1.55}$$

$$V_{ed} = \alpha_d * P^{1.23}$$

$$V_{ef} = \left(1 - 2.5 * 10^{-5} * \sqrt{A_{basin}}\right) * A_{basin} * h * (\alpha_f - 0.24 * 10^{-9} * A_{basin})$$

With the equilibrium volume, the equilibrium concentration of an element can be determined by relating the equilibrium volume and the actual volume of an element. This equilibrium concentration is based on the deviation from the global sediment concentration c_E, which can also be defined as the outside world sediment concentration. This deviation is related to the deviation from equilibrium as defined by comparing the current and equilibrium value of the volume. Since the sediment transport in the ASMITA model is diffusive in nature, the final equilibrium concentrations will all equal the global sediment concentration if a static equilibrium is reached. An element is in a static equilibrium when its volume equals the equilibrium volume of said element. The parameter n in the following formula is the concentration transport exponent, which depends on the type of sediment considered.

$$c_e = C_E * \left(\frac{V_e}{V}\right)^n$$

The change in element volumes follow from the difference between the actual concentration and local equilibrium concentration, multiplied by the area and the exchange rate between the bed. The exchange rate between the bed and water column w depends on the type of sediment considered. Note that depending on the definition of the volume, either sediment or water, the sign of the below formula changes.

$$\frac{dV}{dt} = w * A * (c_e - c)$$

In the ASMITA model sediment transport is considered diffusive, dependant on the gradient of the sediment concentration between two elements multiplied by the horizontal exchange coefficient δ. Disregarding any storage of sediment in the water column this diffusive transport should match the change of an elements volume. In the below formula the subscripts n and m indicate the (equilibrium) concentration of different elements, as now cross element interaction is considered.

$$w * A * (c_{ne} - c_n) = \sum \delta_{n,m} * (c_n - c_m)$$

It has been established amongst others by Van de Waal (2006) and Van Weerdenburg (2019) that there is some residual flow between basins in the Wadden Sea. Including residual flow between elements could be done by adding an advective flow term to the above equation, in which $q_{n,m}$ equals the flow between elements n and m. This formula will be applied in chapter 4 as the base ASMITA model in this chapter is considers diffusive transport only.

$$w * A * (c_{ne} - c_n) = \sum \delta_{n,m} * (c_n - c_m) + q_{n,m} \frac{(c_n + c_m)}{2}$$

Returning to the formula which describes the rate of change of the volume of a model element, this equation does not include sea level rise. Sea level rise can be included as done below, by including the rate of sea level rise multiplied by the model elements area. In this formula dζ/dt describes de rate of sea level rise.

$$\frac{dV}{dt} = w * A * (c_e - c) + A * \frac{d\zeta}{dt}$$

To solve the above functions for all elements and to calculate the corresponding volume changes the following parameters must be known:

- The global equilibrium concentration C_e (-)
- The exchange rate with the bed w (m/s)
- The concentration transport exponent n (-)

- The area of the intertidal flats A_f (km^2)
- The area of the channels A_c (km^2)
- The area of the outer delta A_d (km^2)
- The diffusion coefficient outside world, outer delta δ_{od} (m^3/s)
- The diffusion coefficient outer delta, channel δ_{dc} (m^3/s)
- The diffusion coefficient channel, intertidal flat δ_{cf} (m^3/s)

The ASMITA model allows for modelling with multiple sediment fractions, to account for the presence and difference in behaviour of mud and sand. By defining the change in volume relation for each sediment fraction multiple sediment fractions can be included. Each then has their own global equilibrium concentration, exchange rates and transport exponent.

3.2 ASMITA model setup

The previous section has outlined the ASMITA model formulation and its required parameters. In this section these parameters are defined for each of the basins of the Groningerwad. The average area of the different elements has already been determined as part of the morphological study in the previous chapter (See table 3). The global equilibrium concentration, the concentration transport exponent, and exchange rate with the bed, are sediment characteristics which are the same across the basins of the Groningerwad. The diffusion coefficients depend on sediment characteristics and basin geometry and are determined for each basin. The α parameters of the equilibrium relations are also basin specific.

3.2.1 Sediment characteristics

Two sediment fractions are modelled in these ASMITA models of the Groningerwad. A coarse fraction, resembling sand, and a fine fraction, resembling mud. The sediment characteristics are similar to those applied to a two sediment fraction model of the Zoutkamperlaag basin. And are presented in table 4. The Zoutkamperlaag is the basin adjacent to the Groningerwad on the west. The sediment in the Zoutkamperlaag is slightly finer than the sediment in the Groningerwad due to the shielding of the Zoutkamperlaag by the Schiermonnikoog island. But nevertheless, these are the values applied as determining them outright from field data is quite complex. Furthermore, given the already high level of aggregation and the time span on which is modelled, the difference between sediment characteristics of both areas is not that large. The additional accuracy of relating the sediment characteristics directly to the Groningerwad instead of using those already determined for the Zoutkamperlaag is assumed to be small.

Table 4 Sediment characteristics applied in the ASMITA model.

	Global equilibrium concentration	Concentration transport exponent	Exchange rate with the bed [m/s]
Coarse	0.00040	5	0.015
Fine	0.000015	3	0.00050

3.2.2 Diffusion coefficients

The horizontal exchange coefficients (δ) are based on the sediment characteristics and the geometry of the exchange area between the elements. These horizontal exchange coefficients are based on the dispersion coefficient, the cross element exchange area and an averaged length scale describing the distance between two elements.

$$\delta = D * A_{exchange} / L$$

Where:

$A_{exchange}$ is the cross-sectional area between the two elements

L is a characteristic length describing the distance between the two elements
D is the dispersion coefficient described by the formula below.

$$D = \varepsilon * U^2 * h / w_s$$

Where:
ε = 0.1 is a fitting parameter
U = 1 m/s is the scale of the tidal flow velocity
h is the water depth at the interface between the two elements
w_s is the vertical exchange coefficient of the considered sediment.

For both sediment fractions the exchange coefficients have been determined to be the following based on the latest geometry available from the vaklodingen of 2019 (See also appendix D). Their respective values are presented in table 5 in which the subscripts cf, dc and od represent the exchange coefficients between the channel and flat, delta and channel and the outside world and delta respectively. The subscripts _c or _f denote the coarse or fine fraction.

Table 5 Horizontal exchange coefficients of the basins

	Eilanderbalg	Lauwers	Schild	Sparregat	Ra
δ_{cf_c}	740,6	505,4889	246,8667	111,7366	188,0889
δ_{cf_f}	2,22E+04	1,52E+04	7,41E+03	3,35E+03	5,64E+03
δ_{dc_c}	1,84E+01	2,66E+01	4,02E+01	8,89E+00	2,05E+01
δ_{dc_f}	5,53E+02	7,99E+02	1,20E+03	2,67E+02	6,14E+02
δ_{od_c}	75,13333	183,6	24	34,13333	16,8
δ_{od_f}	2,25E+03	5,51E+03	7,20E+02	1,02E+03	5,04E+02

3.2.3 α parameters of the equilibrium relations

The ASMITA model relies on the equilibrium relations for tidal basins of Eysink (1991). These relations each contain a fitting parameter α, relating either the basin geometry and tidal range to the equilibrium volume of the intertidal flat or the tidal prism to the equilibrium volume of the channel and outer delta. For each basin these fitting parameters differs.

In a situation without sea level rise, finding the α parameters, which relate geometry and tidal prism to the equilibrium values, is quite straightforward. They can simply be deduced from the equilibrium relations and volumes found as part of the morphological study. However, from Vermeersen et al. (2018) we know that the sea level has been rising at an average rate of about 2mm/a. Because of this sea level rise rate, and the fact that the Groningerwad has not been disturbed by major human interventions, the basins of the Groningerwad are assumed to currently be in a dynamic equilibrium state with 2 mm/a of sea level rise.

To determine the α parameters, corresponding to the dynamic equilibrium situation, their values are not calculated directly but fitted. An ASMITA model with the average values of area and volume of each basin with a 2mm/a sea level rise scenario has been set up and supplied with α parameters corresponding to a static equilibrium. A static equilibrium is found from the empirical equilibrium relations when there is no sea level rise. The resulting volumes of the elements after a simulation period of 500 years are then compared to the equilibrium values after which the α parameters are tweaked to ensure that, after the procedure has finished, the resulting volumes after 500 years of simulation, equal the volumes found in the morphological study. This procedure yields the α parameters which are presented in table 6.

Table 6 α parameters of the equilibrium relations

	Eilanderbalg	Lauwers	Schild	Sparregat	Ra
α_f	0.49697	0.56657	0.47166	0.38091	0.45390
α_c	$1.5178 * 10^{-5}$	$1.2042 * 10^{-5}$	$1.2469 * 10^{-5}$	$1.0103 * 10^{-5}$	$5.9671 * 10^{-6}$
α_d	0.011769	0.018892	0.0092532	0.0068496	0.0059996

3.2.4 Sea level rise scenario's

In determining the different α parameters the current sea level rise rate as found by Vermeersen et al. (2018) has already been presented. The further sea level rise scenarios considered in this study are similar to the scenarios applied in the study by Wang & Lodder (2019) presented in figure 17. These are also based on the findings by Vermeersen et al. (2018), which depend on the IPCC predictions concerning sea level rise and climate change presented in their fifth assessment report. All considered sea level rise scenario's start with a value of 2 mm/a. In 2020 then the sea level rise rate accelerates for a period of 30, 40 or 50 years up to a sea level rise rate of either 4, 6 or 8 mm/a respectively. After the acceleration period the sea level rise remains constant at its new level. In addition to these three accelerating scenarios the base 2 mm/a sea level rise rate is also modelled, as well as a 0 mm/a sea level rise scenario for comparison to the static equilibrium. In the labels of the graphs in section 3.3, and figure 17, the different scenarios are denoted as slr0, slr2, slr4, slr6 and slr8 respectively.

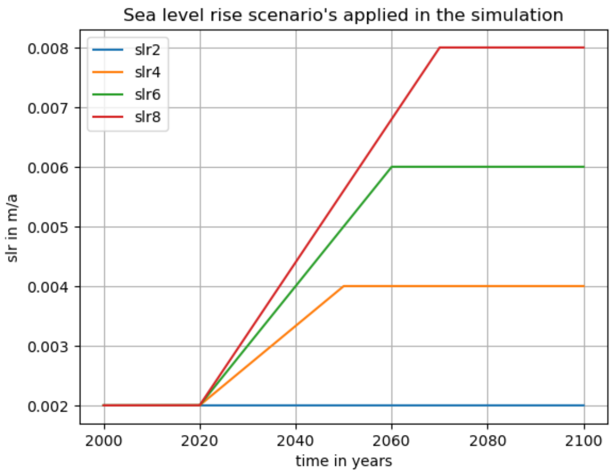

Figure 17 Sea level rise scenarios applied in the ASMITA model based on Vermeersen et al. (2018).

3.2.5 Simulation time

The model set up is similar to that of the set up in the study by Wang & Lodder (2019). The simulations start in 1970 after which there is a 50 year long spin up period. Subsequently in 2020 for the relevant sea level rise scenario's the acceleration of sea level rise starts. This in concordance with the scenarios defined above. The simulation period then further extends for some 450 years.

3.3 Modelling results

The ASMITA model is set up with the information in the previous subsection and the average areas and volumes from the morphological study. It then produces the following results, presented per basin in figures 18-22, in the following six graphs. The first three graphs present the development of volume of the three different elements of the model: the intertidal flat, channel and delta. The fourth graph shows the development of the sediment transport into the basin. This results from subtracting graphs five and six. These two graphs describe the sediment volumes in Mm^3/year retained by the intertidal flat and channel elements. Each graph contains a grey, green, red and purple band. The grey band which starts in 1970 indicates the 50 year spin up time. The remaining green, red and purple bands indicate the acceleration period of the slr4, slr6 and slr8 scenarios respectively.

With the assumption that the basins are currently in dynamic equilibrium with a 2 mm/a sea level rise rate, the 2 mm/a sea level rise scenario shows that volume and transport of the different elements remain constant, as shown in the below results. The fourth graph shows the sediment transport into the basin. It illustrates the difference between static and dynamic equilibrium for the 0 mm/a sea level rise scenarios. The transport develops to 0 a static equilibrium. For the remaining scenarios, the transport develops toward a value which equals the volume change due to sea level rise. In this case a dynamic equilibrium is reached if the graph shows significant asymptotic behaviour. If a graph does not flatten out, then, for that sea level rise scenario, that basin does not develop a new dynamic equilibrium.

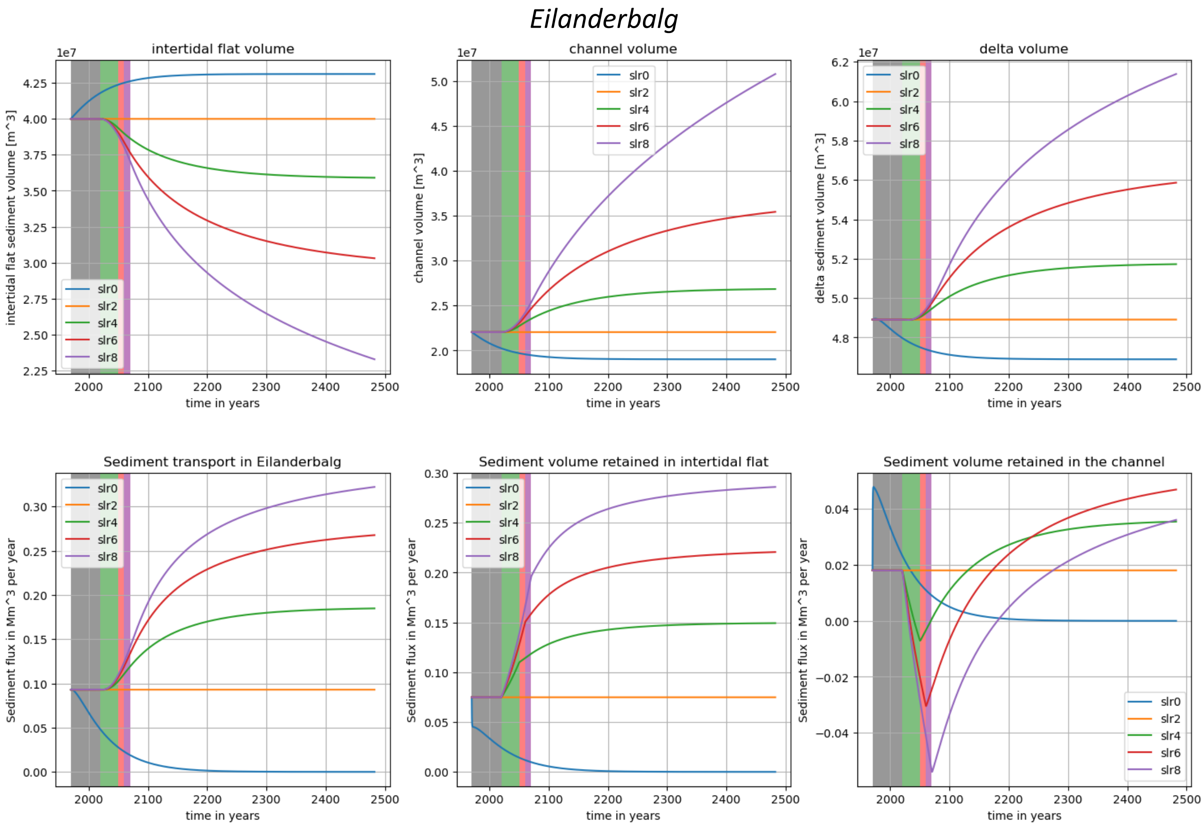

Figure 18 Model results of the Eilanderbalg basin, top left intertidal flat volume, top middle channel volume, top right delta volume, bottom left sediment transport, bottom middle retained volume intertidal flat, bottom right retained volume channel.

Lauwers

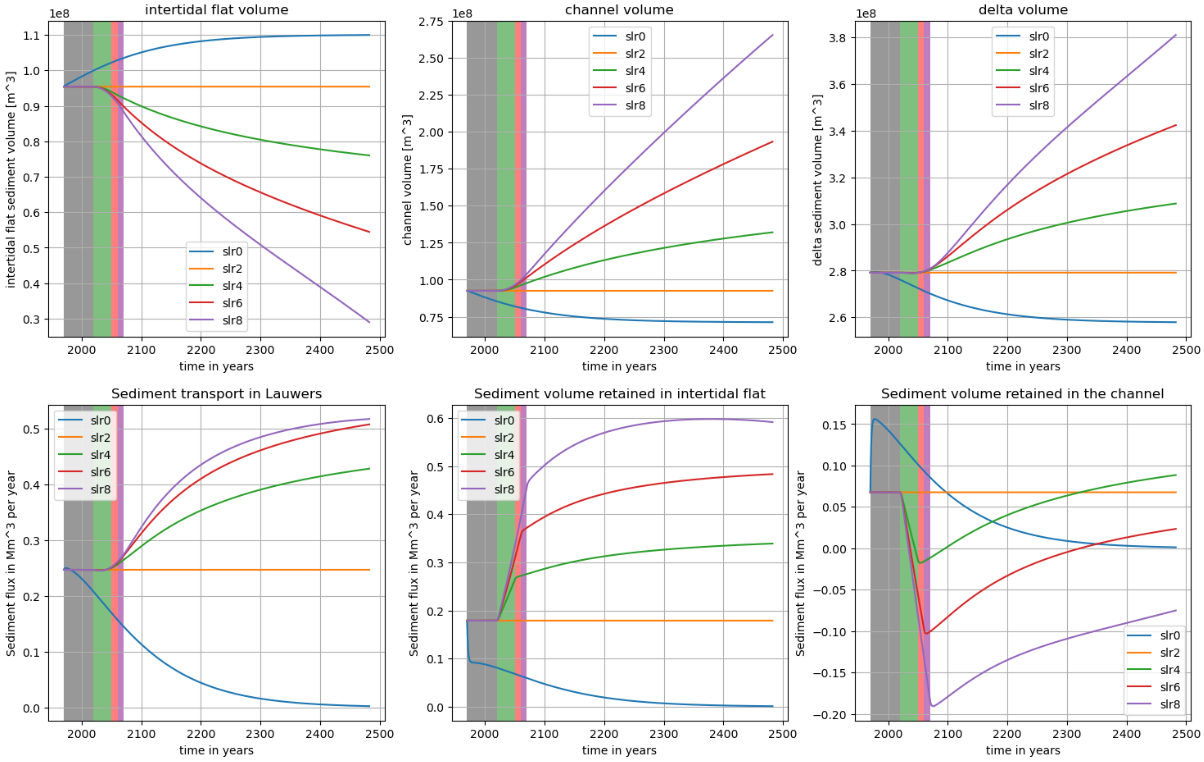

Figure 19 Model results of the Lauwers basin, top left intertidal flat volume, top middle channel volume, top right delta volume, bottom left sediment transport, bottom middle retained volume intertidal flat, bottom right retained volume channel.

Schild

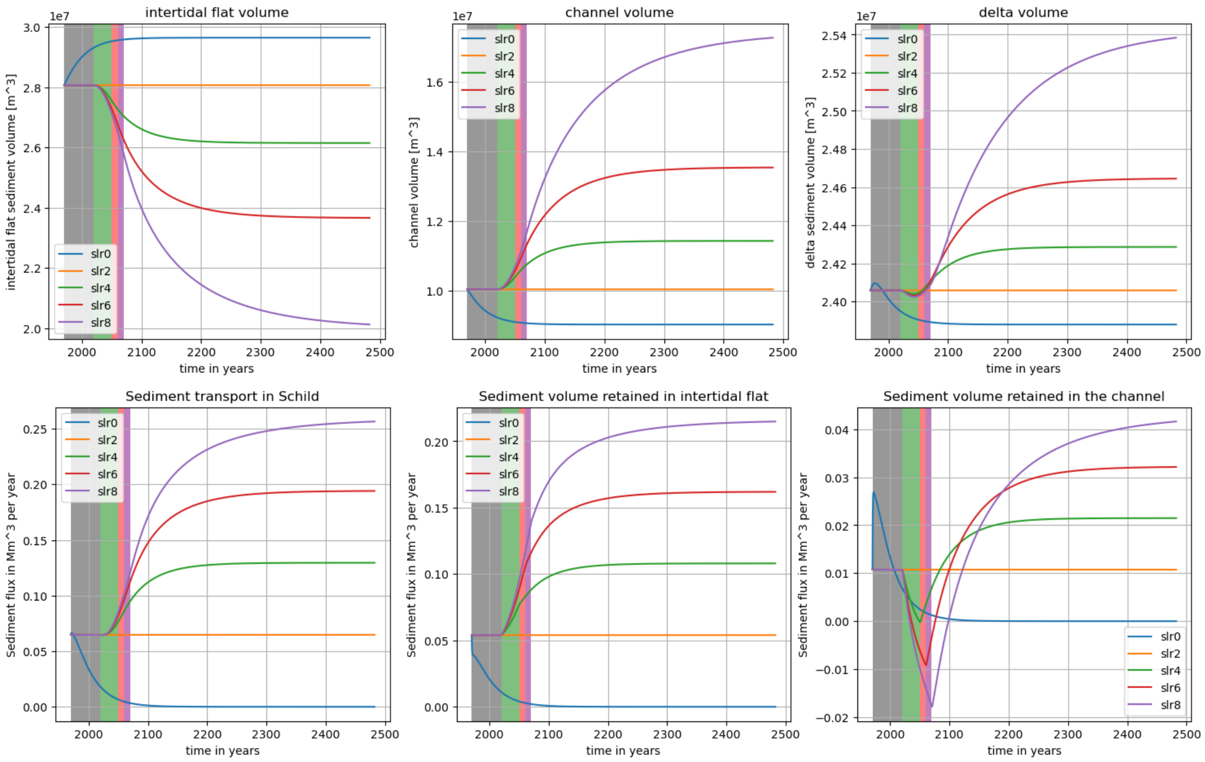

Figure 20 Model results of the Schild basin, top left intertidal flat volume, top middle channel volume, top right delta volume, bottom left sediment transport, bottom middle retained volume intertidal flat, bottom right retained volume channel.

Sparregat

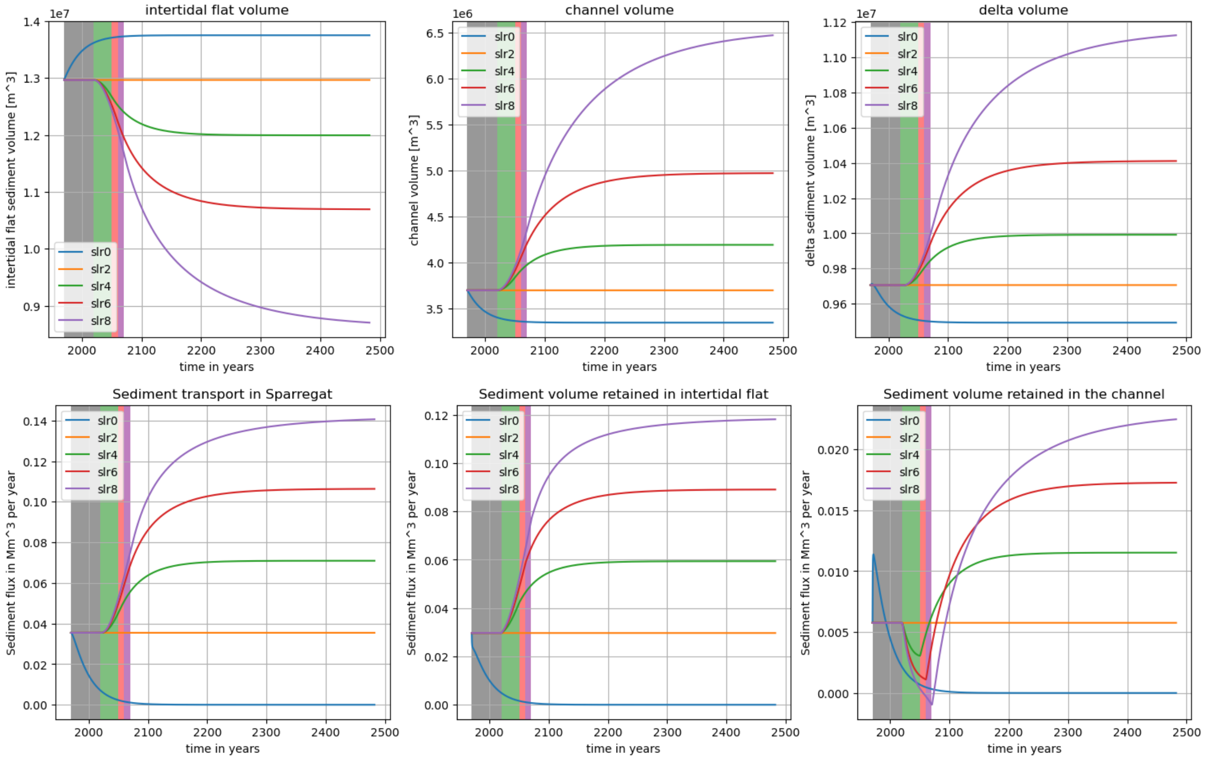

Figure 21 Model results of the Sparregat basin, top left intertidal flat volume, top middle channel volume, top right delta volume, bottom left sediment transport, bottom middle retained volume intertidal flat, bottom right retained volume channel.

Ra

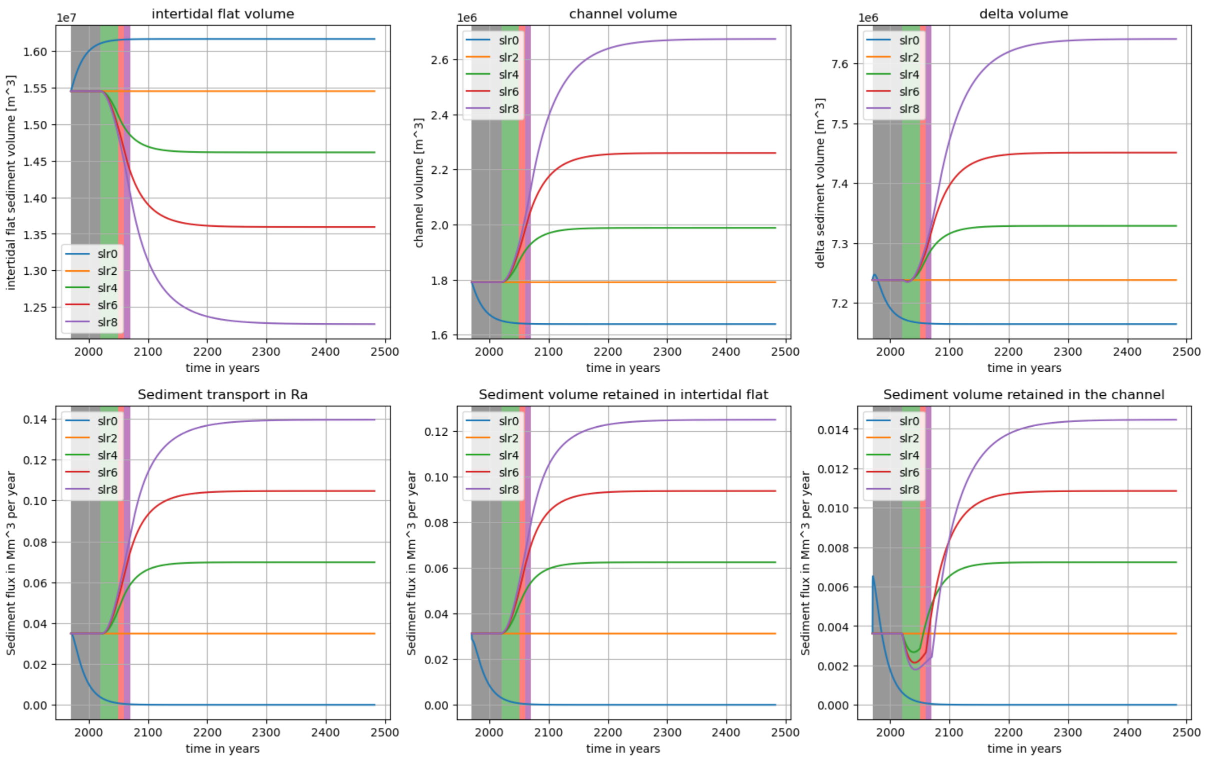

Figure 22 Model results of the Ra basin, top left intertidal flat volume, top middle channel volume, top right delta volume, bottom left sediment transport, bottom middle retained volume intertidal flat, bottom right retained volume channel.

3.3.1 Critical sea level rise

The critical sea level rise rate describes the circumstances for which a basin will drown. The drowning of a basin occurs when the sediment transport is too small to allow for enough sediment import for the basin to match the (accelerating) sea level rise, and all intertidal area is lost. The critical sea level rise rate is the sea level rise rate for which the sediment import exactly matches the volume change induced by sea level rise. Note that even without the sea level rise reaching this critical value already a significant loss of intertidal volume can occur. If the sea level rise rate then accelerates beyond its critical value, no new dynamic equilibrium will be formed which leads to a complete loss of intertidal area. For a three element basin schematisation, as used by the ASMITA model, the critical sea level rise rate is calculated as follows (Wang et al., 2018; Bijsterbosch, 2003; Hinkel et al., 2013):

$$R_c = \frac{C_E}{\frac{1}{w_{sf}} + \frac{A_f + A_c + A_d}{\partial_{od}} + \frac{A_f + A_c}{\partial_{dc}} + \frac{A_f}{\partial_{cf}}}$$

The parameters here are the same as those applied in the ASMITA model, where C_E is the global equilibrium concentration. w_{sf} is the vertical exchange with the bed in the flat element. A_x is the area of element x. And δ_{xy} is the horizontal exchange between elements x, y. In this study a two sediment fraction ASMITA model is applied. For both fractions a critical sea level rise rate can be calculated using the above formulation. The actual critical sea level rise rate for a basin is then found by the sum of the critical sea level rise rate for both sediment fractions. Based on this formulation of the critical sea level rise rate the following values are then found for each basin and presented in table 7.

Table 7 Critical sea level rise rate of the basins of the Groningerwad.

	Eilanderbalg	Lauwers	Schild	Sparregat	Ra
R_c [mm/a]	7.4	4.5	9.9	9.3	12

3.4 Observations and conclusions regarding the modelled results

3.4.1 Assumptions made in the model setup.

The model set up in this study relies on a number of assumptions of which it is important to be aware. Some of these assumptions are inherent to the ASMITA model, such as the choice of the equilibrium formulas, which is therefore not discussed further. Also, the global equilibrium concentration c_E which is the main fitting parameter of the ASMITA model is not considered here as these values for the coarse and fine fraction are taken from the model set up for the Zoutkamperlaag. The assumptions discussed below, however, are the choice of element area and the definition of the α and δ parameters. In general, the values for α and δ are determined by calibrating the model to observed morphological developments. However, for the Groningerwad only six detailed bathymetrical maps, over a period of 30 years, are available. This dataset is unfortunately too short to meaningfully fit the α and δ parameters which is why a different way of determining these values has been chosen as explained in the following sections.

3.4.2 Choice of element area

Within the ASMITA model the area of an element is fixed, it does not change in time. The morphological study however showed that basin area does change over time. As the ASMITA model requires a representative area which does not change, the average area of an element, over the study period of 30 years as determined in chapter 2, was chosen as the element area in the ASMITA model. In general, the results of the morphological study do not show clear trends for the development of basin area for each basin. Furthermore, it is assumed that the basins of the Groningerwad are currently in a dynamic equilibrium state as the system has been relatively unperturbed by human interventions. Because of this, and the fact that there are no clear trends visible, the average area found by the morphological study is chosen as the element area in the ASMITA model.

3.4.3 Definition of α parameters

The definition of the α parameters in this study relies on two mayor assumptions. The first is that the actual sea level rise rate is 2 mm/a. The second is that the basins are in a dynamic equilibrium position state. This second assumption is made because the Groningerwad is relatively unperturbed by human interventions. The first assumption is based on the study by Vermeersen et al. (2018) which found that the current sea level rise for the Dutch coast is about 2 mm/a. For the Groningerwad however this value might very well be wrong given that the sea level rise rate of 2 mm/a does not consider the local effects of gas mining.

The NAM (2016) reported in their plans in 2016 the measured/modelled subsidence caused by gas mining, which is shown in figure 23. It shows that the eastern part of the Groningerwad has been subjected to subsidence due to gas mining. Cleveringa (2008) also reported that the Groningerwad and Ems Dollard area have been subjected to subsidence caused by gas mining. Field observations however have not shown an effect at the surface. This implies that any subsidence in the basins has been covered by importing more sediment. Nonetheless, it is almost certain that in the eastern basins of the Groningerwad locally the relative sea level rise rate (relative as it includes subsidence) has been higher than 2 mm/a. The subsidence due to gas mining is estimated to be about 1.5 mm/a in the Groningerwad. Therefore, the local sea level rise experienced by a basin might be almost twice as large. It should be noted, however, that although locally due to gas mining the sea level rise rate might be larger, the time scales for which the effects of sea level rise are considered are much longer than the time scale for which the effects of gas mining persist.

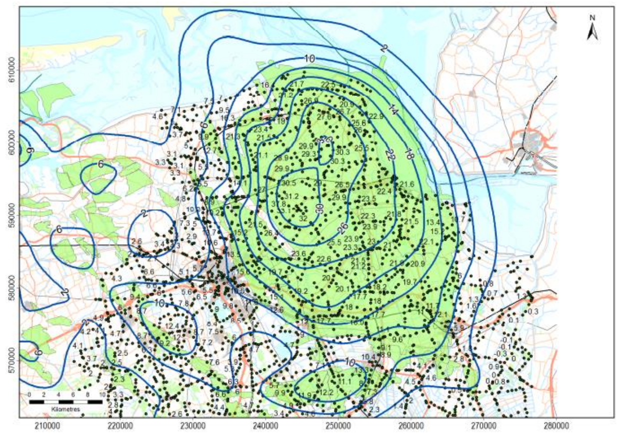

Figure 23 in 2013 measured subsidence and contour lines of modelled subsidence for the period from 1972 to 2013 (NAM, 2016)

3.4.4 Definition of δ parameters

The δ parameters rely on the fitting parameter ε which is set at 0.1. The determination of the horizontal exchange coefficients is difficult in the case of the Groningerwad as there is only 30 years of detailed bathymetric data available. This is a too short time period to meaningfully calibrate the horizontal exchange coefficients. Therefore, the horizontal exchange coefficients are based purely on their underlying formulas as presented in section 3.2.2. The fitting parameter ε is taken from a model for the adjacent basin of the Zoutkamperlaag for which ε = 0.1. In chapter 5 the assumption ε = 0.1 is explored further.

3.5 Conclusion and discussion of the ASMITA model results.

This chapter has addressed the second sub-question: '*What is the projected response of the Groningerwad area for to increasing sea level rise rates?*' By applying the ASMITA model to each of the basins of the Groningerwad with three accelerating and two base sea level rise rates, a projection of response has been made.

Considering the graphs in the result section a number of things stand out. The slr2 scenario with a constant 2 mm/a sea level rise rate is the base case to which the equilibrium parameters have been fitted. This reflects back in the results as for this scenario the volumes and sediment import remain constant throughout the simulation. If the sea level rise rate subsequently increases the volumes of the intertidal flat decrease. This means that intertidal area is lost, and the channel volume increases. The channels thus become larger. With increasing sea level rise rate the delta volume also increases, this is an unexpected result. This increase can be explained, though, as with a decrease of the intertidal area and subsequent increase in the tidal prism and following the equilibrium relations an increase in the equilibrium volume of the delta occurs. However, observations from other modelling exercises (Wang et al., 2020) show that the delta volume should decrease, which, given the context of the situation, is more logical as rising sea level rates induce a larger sediment demand instead of providing more sediment.

More basin specific observations consider the time required to reach a new equilibrium position for the different sea level rise rate scenarios. In general, the results show that it takes a considerable amount of time to reach a new dynamic equilibrium position. The findings presented in the graphs align with the values of the critical sea level rise rate. Showing, amongst other things, that the basin with the lowest critical sea level rise rate, the Lauwers, will take the longest time to reach equilibrium, if it is reached at al. On the other hand, the Ra basin, with the largest critical sea level rise rate, reaches its equilibrium position for all modelled sea level rise scenarios. And it does so quite quickly as well, at least when considering the basins of the Groningerwad. Comparing the results of the Groningerwad with the projections of development of the Wadden Sea presented by Lodder et al. (2022), the Groningerwad appears to react much slower than the smaller basins of the Wadden Sea such as the Pinkegat and Eierlandsegat. This is especially illustrated by the fact that the study by Lodder et al. (2022) presents its results in graphs up to 2100. That show that the Pinkegat and the Eierlandsegat already appear to reach their equilibrium positions with a 4 mm/a sea level rise scenario. The results presented in this study, however, need to consider a time period up to 2470 to get to such a state. Chapter 5 addresses this difference in results between the Groningerwad and the rest of the Wadden Sea further.

Chapter 4 Cross basin flow in ASMITA

The ASMITA model considers a tidal basin as a system through which exchange of sediment only occurs from flat to channel to delta to the outside world. In reality however the basins in the Wadden Sea also exchange sediment between each other. Elias et al. (2012) outlined that the sediment balance of the Wadden Sea cannot be closed without considering cross basin transport of sediment. This chapter aims to explore if an ASMITA model can be setup considering cross basin flow by attempting to model the development of the Zoutkamperlaag and Eilanderbalg basins with between them a cross basin flow. And in doing so aims to answer the third, additional sub-question, '*How does the inclusion of inter basin morphological reaction due to residual flow across the Groningerwad area effect the response to sea level rise?*'

Within the ASMITA model setup there is room to allow for an advective flow term. To explore the effects of cross basin transport the ASMITA model is adapted to consider two basins simultaneously, the Zoutkamperlaag and Eilanderbalg. These two basins are modelled together similar to how a single basin would be considered. But with an added advective flow term flowing between the intertidal flat elements of both basins. In this case from the Zoutkamperlaag to the Eilanderbalg as shown in figure 24. Based on the findings by Elias (2019) the magnitude of this flow is about 0.2 Mm^3/year.

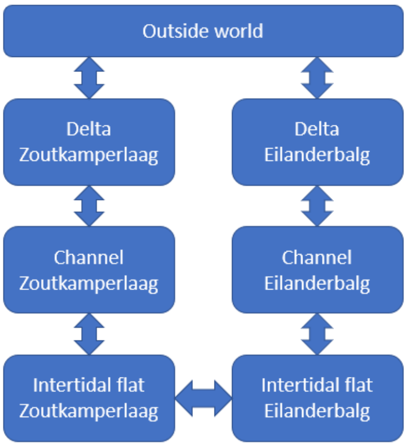

Figure 24 Cross basin flow model set up.

The cross basin flow is modelled as an advective flow term instead of a diffusive term because of the difference in their underlying physical processes. The, unchanged, ASMITA model considers transport into a basin through its inlet where large gross sediment transport occurs every tidal cycle. Thereby a considerably smaller net sediment transport governs basin development. Net sediment transport across the tidal divides is not governed by similar behaviour even though there is some flow of water across the tidal divide every tidal cycle (Van de Waal, 2007). There are only a few conditions where this flow is of the same magnitude as through a basin inlet. These more sporadic events are the cause of sediment transport across a tidal divide. In order to include this sporadic flux across the tidal divide into the ASMITA model, a constant advective term was added to it, of which the yearly volume matches the value found by Elias (2019). Note, however, that the way this advective flow term is currently modelled, is a physically incomplete schematization, as the advective flow term into the flat element is not matched with an advective flow term out. Nonetheless, this model schematization is used to make a first order exploration of the effects of cross basin flow by introducing a sediment flux from the Zoutkamperlaag to the Eilanderbalg.

The advective flow term q has been determined based on the base scenario of 2 mm/a sea level rise similar to how the α parameters were determined. The advective flow term is chosen so that the cross basin transport matches the value of 0.2 Mm^3/year found by Elias (2019), which crosses from the Zoutkamperlaag to the Eilanderbalg. This is shown in figure 25, which also shows that, for the faster sea level rise scenario's, the volume of sediment transported cross basin reduces with accelerating sea level rise.

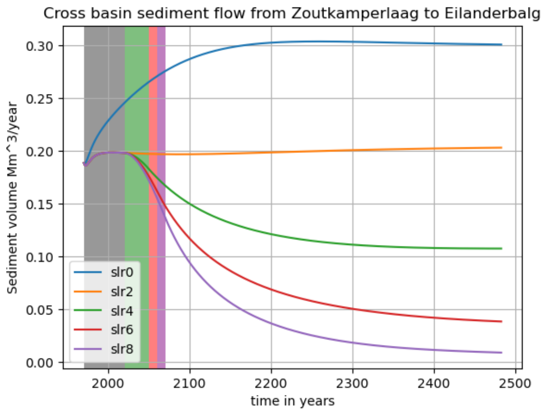

Figure 25 Cross basin sediment flow according to the model set up, fitted to reproduce the 0.2 Mm³ found by Elias for the base 2 mm/y sea level rise scenario.

Modelling the adapted ASMITA model for the remaining sea level rise scenarios produced the results for the Eilanderbalg basin as shown in figure 26. What the graphs show is that considering cross basin transport the 2 and 4 mm/a sea level rise scenario gravitate more towards the static 0 mm/a sea level rise scenario. This is not unexpected as the dynamic equilibrium state relies on a balance between sea level rise and sediment import. An additional sediment transport term into the basin means this balance is found more quickly. This causes the dynamic equilibrium state to be closer to the static equilibrium position. It should be noted, however, that the current equilibrium relations have been fitted to a situation without cross basin flow. Perhaps, if the α parameters are refitted to the new situation, the results will show similar behaviour as the original simulations, without cross basin flow.

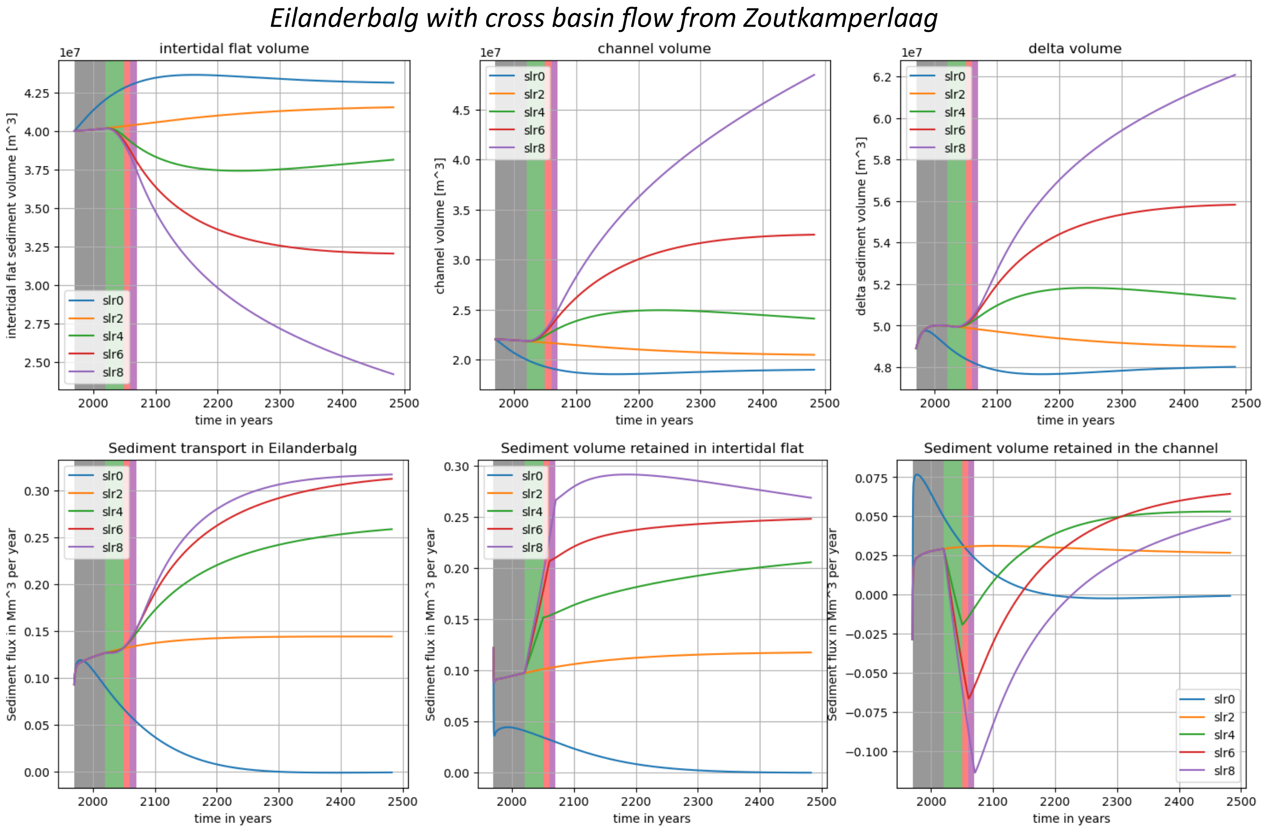

Figure 26 Results of Eilanderbalg model with cross basin flow from Zoutkamperlaag. , top left intertidal flat volume, top middle channel volume, top right delta volume, bottom left sediment transport, bottom middle retained volume intertidal flat, bottom right retained volume channel.

The results of the single basin model of the Eilanderbalg (figure 18) showed that for the 6 mm/a sea level rise scenario and above the basin does not reach a new dynamic equilibrium position. The model which includes cross basin transport shows that for 6 mm/a sea level rise rate a new dynamic equilibrium position is reached. For the 8 mm/a scenario no equilibrium position is reached within the simulation period. This scenario does create an interesting pattern in the sediment transport graphs: an almost similar transport rate for the 8 mm/a sea level rise rate scenario appears as that for the 6 mm/a scenario.

The current set up of this cross basin flow model assumes that the sediment which crosses from the Zoutkamperlaag is all retained in the Eilanderbalg. It is, however, more logical to assume that an eastward directed flux between all basins of the Groningerwad exists. A more accurate representation of the situation would therefore be that not only is there a flux between the Zoutkamperlaag and Eilanderbalg, but also between the Eilanderbalg and Lauwers, Lauwers and Schild etcetera. This approach is not chosen in the current model set up, as this is a first order exploration of the effects of cross basin flow. And the cross basin flow from the Zoutkamperlaag to the Eilanderbalg is known from the study of Elias (2019) whereas the magnitude of a possible flux between the Eilanderbalg and Lauwers is unknown. Therefore, it is difficult to conclude, as done in the previous section, that for the 6 mm/a sea level rise rate scenario, a new equilibrium is indeed reached. This is because any sediment lost by the Eilanderbalg to the Lauwers is omitted. What the results of the model do show is that cross basin transport does influence the dynamic equilibrium position. In this case it is closer to the static equilibrium position. Also, the model results do show that including the cross basin sediment flux means the basins reach a new dynamic equilibrium position sooner. So cross basin transport apparently does have a considerable influence, although the exact effect is still unknown.

Chapter 5 Discussion of results and additional considerations

The main research question of this thesis addresses how the Groningerwad develops with accelerating sea level rise. At the end of this chapter the results of the morphological study and ASMITA modelling are combined in order to make a prediction of how the different basins of the Groningerwad develop. There are however a number of considerations that have come up during this study that are addressed first. These regard the effects of gas mining and basin stability, the methodology of the morphological study, the fitting procedure of the relevant parameters of the ASMITA model, and a comparison of results with other Wadden Sea basins.

5.1 Additional considerations based on results and findings.

5.1.1 Effects of gas mining and basin stability

Gas mining has already been introduced as a relevant process in the Groningerwad area effecting the relative sea level rise by causing subsidence in chapter 3.4.3. This effect locally causes a relative sea level rise rate larger than the 2 mm/a which in this study is taken as the base case (see figure 23 and chapter 3.4.3). Subsidence caused by gas mining is an effect with a shorter time span than the time period over which the effects of sea level rese is considered. Therefore, the effect of gas mining is disregarded in the model set up. This however does not mean that gas mining has no effect at all.

The basin most effected by gas mining subsidence is the Ra, followed by the Sparregat and Schild which are almost completely within the 2 mm subsidence contour line of modelled subsidence for the period from 1972 to 2013 (NAM, 2016). When determining the effects of gas mining on basin stability the proximity of the Groningerwad basin to their equilibrium position, based on the normalised hypsometric curves in chapter 2.2.1, is considered. Based on these hypsometric curves it was found that the Eilanderbalg and Lauwers basins are closest to their equilibrium position, and the Ra and Sparregat basins are furthest off their equilibrium position (see chapter 2.2.2). Consequently it might be possible that, due to gas mining activities the basins in the eastern part of the Groningerwad (Schild, Sparregat, Ra) have moved away from their equilibrium position, as shown in their hypsometric curves. At least more so than the Eilanderbalg and Lauwers basins in the western part of the Groningerwad, as the hypsometric curves of the Eilanderbalg and Lauwers show a smaller spread (See also appendix C for the hypsometric curves). It might be possible that due to gas mining the spread in the hypsometric curves of the eastern basins has become larger, however, since there is no detailed bathymetrical data available from before the start of the gas mining activities, it is impossible to prove if this is actually the case.

5.1.2 Methodology of the morphological study

The procedure applied in the morphological study to determine the boundaries of the ebb tidal delta has produced results with a much larger spread than the procedure applied to determine the basin boundaries, see appendix E in addition to the results in chapter 2. The 'komberginsrapport Lauwers en Groningerwad' of Elias and Cleveringa (2021) does report large changes in the outer delta. However, it should still be noted that the results of the morphological study are prone to errors. Especially the outer delta of which the boundaries are more difficult to determine from the bathymetry. Also, the volume definition of the ebb tidal delta relies on an uninterrupted reference beach profile. To create this reference beach profile the formula and parameter was fitted to data from the Ameland beach profile. It is assumed here that the beach profile of Ameland is similar to an uninterrupted beach profile in the Groningerwad. Ameland does not border the Groningerwad but is one island over. Its general orientation, though, is quite similar to that of the Groningerwad.

5.1.3 Fitting procedure of relevant parameters in the ASMITA modelling and comparison with different basins in the Wadden Sea

The general procedure applied when determining relevant parameters, in this case the horizontal exchange coefficients between the basin elements and the α parameters of the equilibrium relations, consists of a calibration component in which the values are adapted in such a way that modelling results match the developments of real world, or at least those that were measured. In this study such a calibration for the horizontal exchange coefficients and α parameters has not been performed. This is because the available bathymetric data does not provide clear trends over a large enough timespan to meaningfully fit any of these parameters.

This study has worked around this problem by determining the horizontal exchange coefficients purely on their underlying formulas. To that extent the fitting parameter ε was not edited. With these values the modelled sediment transport into the different basins is of the order of 0.1 Mm^3 for the 2 mm sea level rise scenario. Comparing this to the values presented by Elias (2019) the general throughput of a tidal inlet in the Wadden Sea is of the order of 1 Mm^3. Also, the cross basin transport from the Zoutkamperlaag to the Eilanderbalg is, with a magnitude of 0.2 Mm^3, already twice as large as the modelled transport through the Eilanderbalg inlet.

The critical sea level rise rates determined for each of the basins of the Groningerwad is also relatively small compared to critical sea level rise rates of other small Wadden sea basins. The Pinkegat, Eierlandsegat and Zoutkamperlaag have, according to Wang et al. (2018), critical sea level rise rates of 32.7, 18.0 and 17.1. These are all larger than the values found for any of the basins of the Groningerwad, of which most, if not all, have a smaller area.

It is to be expected that the transport into the basins of the Groningerwad is smaller than that of the transport into other basins of the Wadden Sea as the Groningerwad basins are considerably smaller. The difference is, however, quite considerable. Note, though, that the Eierlandsegat does show a similar magnitude of transport as seen in the Groningerwad even though the Eierlandsegat exports instead of imports sediment.

The findings of the previous paragraphs would lead us to believe that the horizontal exchange coefficients in reality are larger than the values currently applied in the model. Unfortunately there is not enough available bathymetrical data over a long enough time period to perform a calibration procedure for the horizontal exchange coefficients. Consequently, it should be emphasized that interpretation of the modelled results, because of these comparisons between sediment transport and critical sea level rise rates between the Groningerwad and the Wadden sea, are to be considered carefully.

Due to the lack of available bathymetrical data the α parameters of the equilibrium relations are not calibrated towards measurements. Instead, they are chosen to produce the average volume for the base level of sea level rise of 2 mm/a, as explained in chapter 3. In that chapter also the effect of gas mining on the accuracy of the α parameter has been addressed. Had more data been available, another method of choosing (calibrating) these parameters would have been chosen.

5.1.4 What if the horizontal transport coefficients are larger?

When comparing sediment transport patterns in the Wadden Sea with the modelled results for the Groningerwad an interesting fact appears. Taking into consideration the difference in critical sea level rise rate found for the Wadden Sea basins and the Groningerwad, as done in the previous section, it appears to be the case that the horizontal transport coefficients are too small. As mentioned, due to a lack of available bathymetrical data it is difficult to meaningfully fit the parameter ε to produce more realist results. It is, however, possible to explore a short what if scenario. Given the observation that sediment transport rates and the critical sea level rise rates are small for the Groningerwad, what if the horizontal transport coefficients would be larger?

For this hypothetical simulation ε = 0.2 is chosen instead of 0.1. Consequently, the horizontal exchange coefficients are twice as large. Performing a simulation for the Eilanderbalg basin similar to the simulation performed in chapter three. The only difference is the increase in horizontal exchange coefficients. The results of this simulation are presented in figure 27.

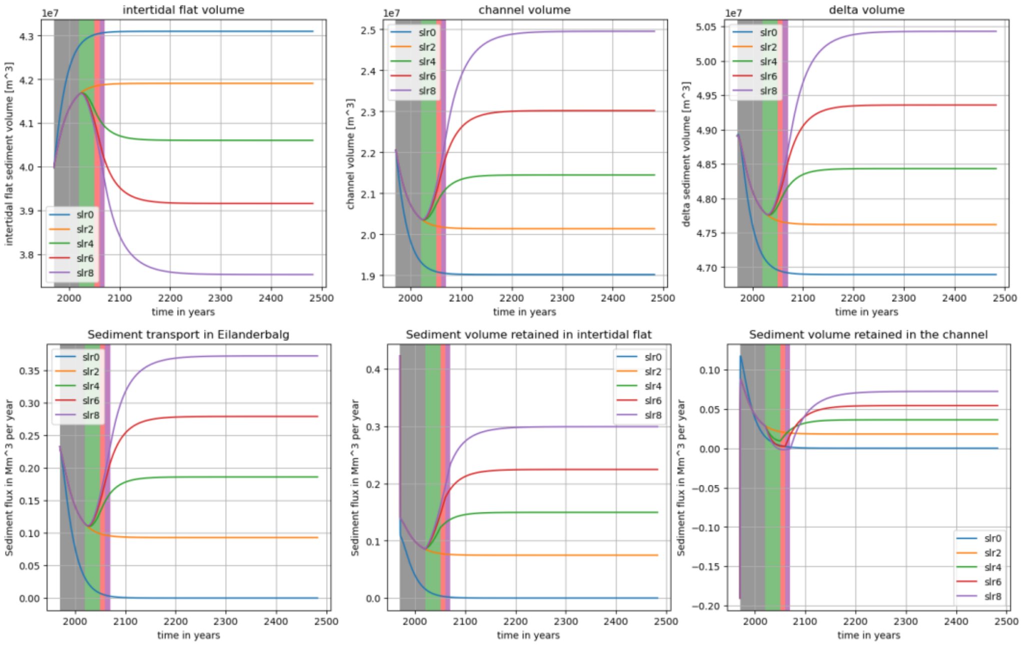

Figure 27 Results of Eilanderbalg simulation with increased horizontal exchange coefficients, top left intertidal flat volume, top middle channel volume, top right delta volume, bottom left sediment transport, bottom middle retained volume intertidal flat, bottom right retained volume channel.

Comparing the above graphs of figure 27 with the simulation results of chapter three (figure 18), the 2 mm/a sea level rise rate scenario does not start within its dynamic equilibrium position anymore. This is not an unexpected finding as the α parameters of the empirical equilibrium relations are fitted to represent the dynamic equilibrium state with the horizontal exchange coefficients determined with $\varepsilon = 0.1$. Larger horizontal exchange coefficients result in a larger sediment transport capacity which means that the dynamic equilibrium position lies closer to the static equilibrium position (0 mm/a sea level rise). Similar to the results presented in figure 26 in chapter 4, more transport means that the dynamic equilibrium position lies closer to the static equilibrium regardless of the source of the additional sediment.

With an increase in ε from 0.1 to 0.2 also the critical sea level rise rates increase with factor 2, as shown in table 8. This is still smaller than some of the critical sea level rise rates found for other Wadden Sea basins by Wang et al. (2018). As mentioned, lack of available data makes it difficult to assess what the actual horizontal exchange coefficients should be. It is however quite realistic that the actual horizontal exchange coefficients could be larger than those used in chapter three of this study.

Table 8 Critical sea level rise rates with increased horizontal exchange coefficients

	Eilanderbalg	Lauwers	Schild	Sparregat	Ra
R_c [mm/year] for $\varepsilon = 0.1$*	7.4	4.5	9.9	9.3	12
R_c [mm/year] for $\varepsilon = 0.2$	15	8.8	20	19	23

(* As stated before in table 7)

5.2 Discussion of results and prediction of development of the Groningerwad

Based on the findings of the morphological study and the modelling results the following predictions are made regarding the development of the Groningerwad. The development of the basins is treated from west to east.

5.2.1 Predictions of development - Eilanderbalg

The Eilanderbalg basin is considered the most stable basin of the Groningerwad based on the hypsometry determined as part of the morphological study. The Schiermonnikoog island, which borders the Eilanderbalg has over the study period expanded eastward. Assuming this expansion continues, and the Eilanderbalg remains in its stable state. It will likely move eastward along with the eastward growth of the island. When introducing accelerating sea level rise, in the ASMITA model, the model results showed that the Eilanderbalg has difficulty forming a new dynamic equilibrium state for the 6 mm/a scenario (although the critical sea level rise rate indicated that over a longer timespan a new equilibrium state would have been reached). Consequently, for low levels of the increase of sea level rise rate, the development as just outlined is not expected to change much. Larger levels of the increase of sea level rise rate would probably halt eastward expansion and have the basin yield area to the Zoutkamperlaag, the basin bordering the Eilanderbalg to the west. Since the critical sea level rise rate of the Lauwers is lower than that of the Eilanderbalg it is unlikely that with increasing sea levels the Lauwers would become larger at the expanse of the Eilanderbalg. Should extreme levels of sea level rise occur, the Eilanderbalg basin will likely drown.

5.2.2 Predictions of development – Lauwers

The morphological study found that currently the area of the Lauwers is reducing. This is at the expense of the Schild and Eilanderbalg basins. This behaviour is likely to continue with the Eilanderbalg pushing from the east, and the eastward movement of Schiermonnikoog. Also of influence is the developing Schild basin on the west. The Lauwers basin is almost squeezed, between the Schild and Eilanderbalg, and this is likely to continue especially if the sea level rise rate accelerates. The ASMITA model of the Lauwers shows that, for even the lowest acceleration considered, the Lauwers basin does not reach a new dynamic equilibrium position. It is therefore highly likely that, with accelerating sea level rise rates, the Lauwers will become smaller at the expense of the Eilanderbalg, Schild and perhaps Ra basins. With extreme conditions of sea level rise this predicted loss of area will be mostly to the Schild and Ra basins, as their critical sea level rise rate is larger than that of the Eilanderbalg. The Rottumerplaat Island will likely move toward the mainland coast at the expanse of the Lauwers basin. Therefore, with acceleration of the sea level rise rate, the area will either be reduced by the adjoining basins or, if that is not the case, it will almost certainly drown.

5.2.3 Predictions of development – Schild

The Schild basin has over the last 30 years developed and increased in area. This expansion is likely to continue. This will largely be at the expense of the Lauwers which is decreasing in area currently. The Sparregat has remained mostly constant in area next to the Schild basin. With accelerating sea level rise this behaviour will likely continue. ASMITA modelling results showed that only for the most extreme sea level rise scenario of 8 mm/a the Schild basin does not reach a new dynamic equilibrium. Given that the critical sea level rise rate of the Schild and Sparregat are almost similar, whereas that of the Lauwers is smaller, it is expected that with accelerating sea level rise the Schild basin will likely gain some area from the Lauwers. Only in the most extreme scenario will the Schild basin actually drown.

5.2.4 Predictions of development – Sparregat

The Sparregat, although not the most stable basin considering the hypsometry has retained the most stable area during the 30 years which are considered in the morphological study. Bordered by the developing Schild in the east and Ra in the south, this basin is expected to remain in its current state. Perhaps, if the spread in hypsometry is indeed caused by gas mining activities, a more stable position of morphological equilibrium will be reached when the mining in Groningen stops. Considering sea level rise, the ASMITA modelling showed similar results for the Sparregat as for the Schild basin. A new equilibrium emerges for all but the most extreme considered sea level rise scenario. With the critical sea level rise of the Sparregat being just a bit smaller than that of the Schild, in the case of extreme sea level rise the Sparregat might lose a bit of area to the Schild basin. This is more likely at the border with the Ra basin in the south which has an even larger critical sea level rise rate. In the most extreme cases, where also the Rottumerplaat island might move more towards the mainland coast, the situation can occur, the Sparregat will drown.

5.2.5 Predictions of development – Ra

The Ra basin has, just like the Sparregat, remained mostly constant in area although, based on the hypsometry is not as stable as the other basins of the Groningerwad. Again, gas mining might have an effect here, although that is difficult to proof. Possibly, due to the small size of the Ra combined with a relatively large channel area, this basin has the largest critical sea level rise rate of all basins. The ASMITA modelling showed that the Ra basin reaches a new equilibrium position for all sea level rise scenarios. It will probably grow in area at the expanse of the tail of the Lauwers basin, and, in the very extreme conditions it might also grow at the expanse of the Sparregat in the north.

5.2.6 Summary of predicted development

The predicted movement of the tidal divides between the different basins has been drawn in figure 28 in the map of the bathymetry in 2019. The white arrows show the predicted movement of tidal divides. The black arrows the predicted movement of islands. From the morphological study it is known that the Schiermonnikoog islands develops eastward. And the Rottumerplaat and Rottumeroog islands move landwards. It is assumed this behaviour will continue in the future.

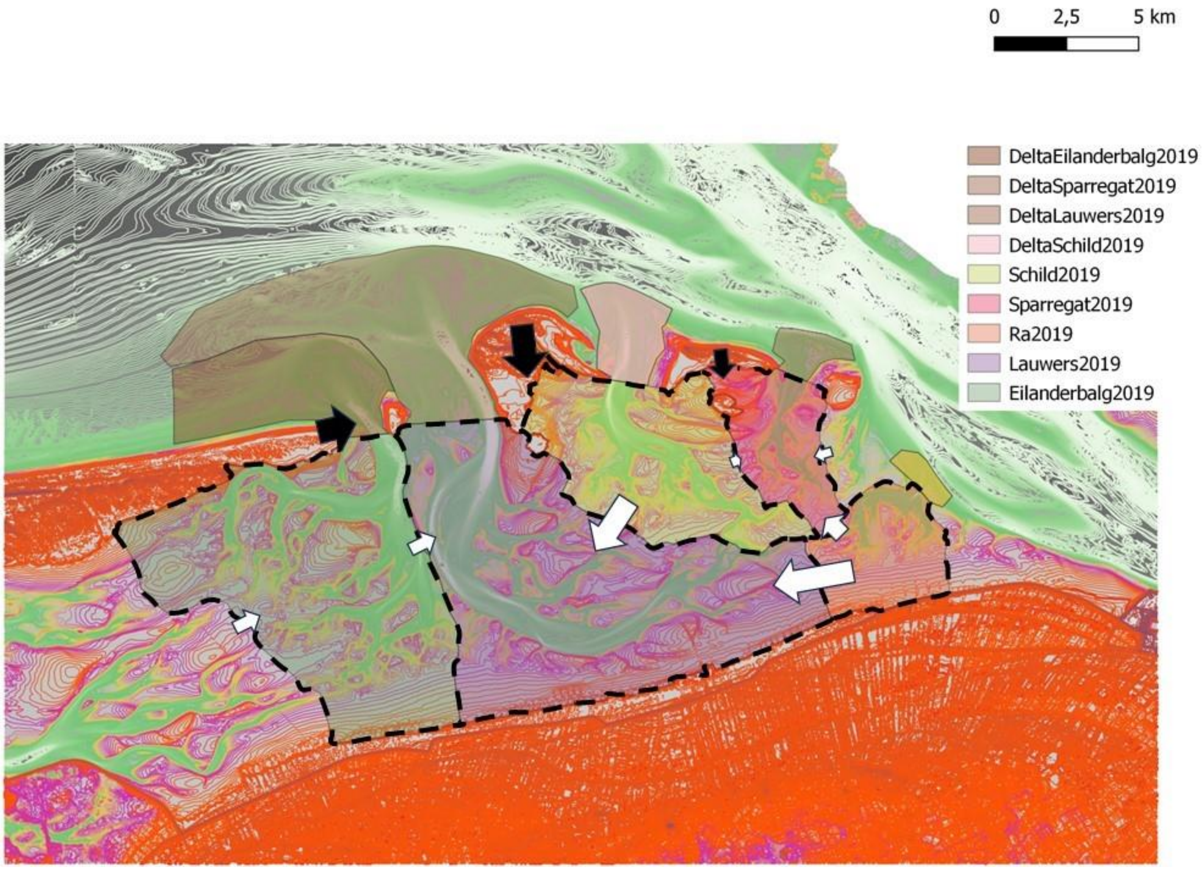

Figure 28 Prediction of movement of tidal divides (white arrows), and islands (black arrows), in the Groningerwad.

Chapter 6 Conclusion and recommendation

To determine how the Groningerwad develops under sea level rise a morphological study and ASMITA modelling of different sea level rise scenarios has been performed. This concluding chapter aims to bring together all these findings.

6.1 Conclusion

The literature review of the morphological study found that the Groningerwad is dynamic area containing highly migratory channels. It consists of five tidal basins, from west to east the Eilanderbalg, Lauwers, Schild, Sparregat and Ra. In the past 30 years the Eilanderbalg and Lauwers have been the most morphodynamically active basins. The Schild in this period has developed to a fully fletched basin. Whereas the Sparregat and Ra have remained mostly constant in area. The Groningerwad also consists of two islands, Rottumerplaat and Rottumeroog which have moved more landward during this 30 year period. The Schiermonnikoog island, which borders the Groningerwad, has developed towards the east.

The analysis of bathymetrical data found similar findings to previous observations (Cleveringa, 2008; Vermaas & Marques, 2017, Elias & Cleveringa, 2021). The total area of the basins within the Groningerwad has decreased over the study period. The Lauwers basin has decreased in its area to the benefit of the Schild, which has shown a steady increase in area. The Eilanderbalg remained more or less constant in area until a subchannel of the Lauwers migrated to the Eilanderbalg which considerably increased its area. The Sparregat and Ra retained more or less the same area during the study period.

An assessment of each basins proximity to their equilibrium position was made using hypsometric curves made of the different basins. Based on these graphs it was concluded that the Eilanderbalg and Lauwers basins are closest to equilibrium. The Sparregat and Ra the furthest of it with the Schild basin somewhere in between. However, because of the normalisation applied in making these hypsometric curves, information on volume is lost and this should be considered when interpreting this result.

An ASMITA model has been set up for each of the five basins. The average volumes of the different elements of the basin found as part of the morphological study were used as starting values. The model consists of a coarse and fine sediment fraction. The α (fitting) parameters of the different empirical equilibrium relations that form the basis of the ASMITA model have been fitted by assuming a dynamic equilibrium state for the current 2 mm/a sea level rise rate. The horizontal exchange coefficients (δ) between the elements of the model have been calculated from their respective formulas and the geometry of the different basins.

With this setup the ASMITA model has predicted how the basin will develop under five different scenarios of sea level rise, ranging from 0 mm/a to 8 mm/a. The model results ran for a simulation period of 500 years. From this simulation the following conclusions arise. The Ra basin develops toward a new dynamic equilibrium for all sea level rise scenarios. The Schild and Sparregat basins develop toward a new dynamic equilibrium for all scenarios except the 8 mm/a scenario. The Eilanderbalg basin reaches a new dynamic equilibrium for the 4 mm/a scenario. And the Lauwers does not appear to develop toward a new dynamic equilibrium. These model observations align with each basins critical sea level rise rate which is smallest for the Lauwers basin and largest for the Ra.

Combining the results of the morphological study and the ASMITA modelling the following predictions are made regarding the development of the Groningerwad. As the area of the Groningerwad has over time been decreasing, this behaviour is expected to continue which means that the Rottumerplaat and Rottumeroog islands will move more landward. The Lauwers basin which has the smallest critical sea level rise rate will most likely decrease in area at the expense of the Schild and Eilanderbalg basin. The Ra basin, which has the largest critical sea level rise rate, will most likely gain area at the expense of the Sparregat and also of the tail end of the Lauwers. The Eilanderbalg basin will most likely continue developing eastward along with the Schiermonnikoog islands. In the more extreme scenarios the Eilanderbalg will likely lose a lot of intertidal Area. The Schild which has been steadily expanding at the expense of the Lauwers will likely continue to do so. The Schild as well as the Sparregat form a new dynamic equilibrium for all but the most extreme sea level rise scenarios. So, both basins will be able to keep up with a considerable acceleration of sea level rise. The Sparregat will likely remain stable in area perhaps losing some area to the Ra and moving more landward together with the Rottumeroog.

6.2 Recommendation based on results and corresponding assumptions.

To perform the ASMITA modelling a number of assumptions have been made. The most important of those regard finding the α and δ parameters. In the case of the α parameters this relies heavily on the assumption of dynamic equilibrium. For the underlying formulation of the horizontal exchange coefficients that in these formulas the fitting parameter $\varepsilon = 0.1$.

The reason these two assumptions have been made is due to the lack of available bathymetric data. The available data for the morphological study entails a period of 30 years. Given the time span that the ASMITA model considers, this was deemed too short to meaningfully fit either the α or ε parameters. This is a large weakness in this study, which especially becomes apparent when comparing the transport patterns in the Wadden sea with the results of this study. The cross basin sediment flow to the Eilanderbalg of 0.2 Mm^3, found in the study by Elias, is much larger than the sediment flow across the inlet of the Eilanderbalg of only 0.1 Mm^3 as modelled in this study. The sediment transport patterns found in the Wadden sea are also considerably larger, as well as the critical sea level rise rates of other basins of the Wadden Sea compared with the basins of the Groningerwad. A what-if-scenario performed in this study also showed that with larger horizontal exchange coefficients, the critical sea level rise rates increase, and the basins show a faster response towards a new dynamic equilibrium. Therefore, it is recommended to reconsider this study at a later time when more bathymetric data is available. This in order to more accurately fit the relevant parameters. The continuous measurement campaigns of Rijkswaterstaat will likely produce this information in the years/decades to come.

References

Bosboom, J. and Stive, M.J.F. (2021). Coastal dynamics. *Delft University of Technology, Delft, The Netherlands.* Revision no. 1269 logged at 2021-01-21 09:13

Bijsterbosch, L.W.W. (2003). Influence of relative sea level rise on tidal inlets. MSc Thesis. Delft University of Technology – report Delft Hydraulics (Delft).

Cleveringa, J. (2008). Ontwikkeling sedimentvolume Eems-Dollard en het Groningerwad: Overzicht van de beschikbare kennis en gegevens. Rapport A2269R1r3 (in Dutch). Alkyon, Marknesse, 47 pp.

Deltaprogramma Kust (2014). Beslissing zand: Geen zand, geen land! Adaptatie agenda voor duurzaam behoud van de kust. Deltaprogramma Waddengebied en deltaprogramma Zuidwestelijke Delta.

Dillingh, D. (2013). Kenmerkende waarden Kustwateren en Grote Rivieren, Deltares rapport 1207509-000-ZKS-0010, versie 4, 6 november 2013. http://publicaties.minienm.nl/documenten/kenmerkende-waarden-kustwateren-en-grote-rivieren

Elias, E.P.L., van der Spek, A. J. F., Wang, Z. B., De Ronde, J. (2012). Morphodynamic development and sediment budget of the Dutch Wadden Sea over the last century. Geologie En mijnbouw/Netherlands Journal of Geosciences, 91(3), 293–310. https://doi.org/10.1017/S0016774600000457

Elias, E.P.L. (2019). Een actuele sedimentbalans van de Waddenzee. Rapport 11203683-001, Deltares, Delft

Elias, E.P.L., Wang, Z.B. (2020). Synthese sedimentbalans Waddenzee. Rapport 1220339-007, Deltares, Delft

Elias, E.P.L., Cleveringa J. (2021). Komberginsrapport Lauwers en Groningerwad. Rapport 11206799-002, Deltares, Delft

Eysink, W. D. (1991). Morphologic response of tidal basins to changes. The Dutch Coast: Paper No. 8.

Hinkel, J., Nicholls, R.J., Tol, R.S.J., Wang, Z.B., Hamilton, J.M., Boot, G., Vafeidis, A.T., McFadden, L., Ganopolski, A., Klein, R.J.T. (2013). A global analysis of erosion of sandy beaches and sea-level rise: an application of DIVA. Global and Planetary Change 111: 150–158

Huismans, Y., Van der Spek, A., Lodder, Q., Zijlstra, R., Elias, E.P.L., Wang, Z.B. (2022). Development of intertidal flats in the Dutch Wadden Sea in response to a rising sea level: spatial differentiation and sensitivity to the rate of sea level rise. Ocean Coast Manag., 216 (2022), Article 105969, https://doi.org/10.1016/j.ocecoaman.2021.105969

Lodder, Q.J., Wang, Z.B., Elias, E.P.L., van der Spek, A.J.F., de Looff, H., Townend, I.H. (2019). Future response of the Wadden Sea tidal basins to relative sea-level rise—an aggregated modelling approach. Water 11 (10). https://doi.org/10.3390/w11102198.

Lodder, Q.J., Huismans, Y., Elias, E.P.L., De Looff, H., Wang, Z.B. (2022). Future sediment exchange between the Wadden Sea and North Sea coast - insights based on ASMITA modelling. Special issue future Dutch coast Ocean Coast Manag, 219 (2022), Article 106067, https://doi.org/10.1016/j.ocecoaman.2022.106067

Ministerie van infrastructuur en waterstaat (2021). Nationaal Deltaprogramma 2022 iedere shop in de grond klimaatbestendig

NAM (2016). Winningsplan Groningen Gasfield 2016

Nederhoff, K., Smits, B., Wang, Z.B. (2017). KPP Wadden, Data analyse: getij en morfologie. Rapport 11200521-000-ZKS-0002, Deltares, Delft

Rijkswaterstaat, (1994). Tienjarig overzicht 1981-1990: presentatie van afvoeren, waterstanden, watertemperaturen, golven en kustmetingen. ISBN 9036900646

Stive, M.J.F., Roelvink, J.A., De Vriend, H.J. (1990). Large-scale coastal evolution concept. In: Louisse, C.J., Stive, M.J.F. & Wiersma, J. (eds): The Dutch coast; report of a session on the 22nd International Conference on Coastal Engineering 1990, Paper 9: 13 pp

Townend, I., Wang, Z. B., Stive, M., Zhou, Z. (2016). Development and extension of an aggregated scale model: Part 1–background to ASMITA. China Ocean Engineering, 30(4):483–504.
Van der Spek, A.J.F., Beets, D.J., 1992. Mid-Holocene evolution of a tidal basin in the western Netherlands: a model for future changes in the northern Netherlands under conditions of accelerated sea-level rise? Research Conference on Quaternary Coastal Evolution 80 (3), 185–197. https://doi.org/10.1016/0037-0738(92)90040-X

Van de Waal, R. (2007). Sediment transport patterns in the Dutch Western Wadden Sea [Master thesis, TU Delft]. Educational repository. http://resolver.tudelft.nl/uuid:97880f59-78ac-4f5a-aa7f-bff8da1b10fb

Van Goor, M. A., Zitman, T. J., Wang, Z. B., Stive, M. J. F. (2003). Impact of sea-level rise on the morphological equilibrium state of tidal inlets. Marine Geology, 202(3–4), 211–227. https://doi.org/10.1016/S0025-3227(03)00262-7

Van Weerdenburg, R., (2019). Exploring the relative importance of wind for exchange processes around a tidal inlet system: the case of Ameland Inlet [Master thesis, TU Delft]. Educational repository. http://resolver.tudelft.nl/uuid:a0e9e030-0feb-4977-bfcd-2a324a6c65c1

Vermaas, T., Marges, V. (2017). Volumeanalyse Oostelijke Waddenzee. Rapport 1230043- 003, Deltares, Delft

Vermeersen, L.L.A., Slangen, A.B.A. et al. (2018). Sea level change in the Dutch Wadden Sea. Netherlands Journal of Geoscience, Netherlands Journal of Geosciences, 97-3: 79-127.

Wang, Z.B., Elias, E.P.L., Van der Spek, A.J.F., Lodder, Q.J. (2018). Sediment budget and morphological development of the Dutch Wadden Sea: impact of accelerated sea-level rise and subsidence until 2100. Netherlands Journal of Geoscience, Netherlands Journal of Geosciences, 97 – 3: 183–214.

Wang, Z.B., Lodder Q.J. (2019). Sediment exchange between the Wadden Sea and North Sea Coast. Modelling based on ASMITA. Rapport 1220339-008-ZKS-006, Deltares, Delft

Wang, Z.B., Huismans, Y., Van der Spek, A.J.F. (2020). Morphological development of the tidal inlet systems in the Wadden Sea. Rapport 11203724-012-BGS-0002, Deltares, Delft

Westerhoff, W.E., Cleveringa, P., (1990). sea-level rise and coastal sedimentation in central noord-holland (The Netherlands) around 5000 BP: a case study of changes in sedimentation dynamics and sediment distribution patterns. In: Beukema, J.J., Wolff, W.J., Brouns, J.J.W.M. (Eds.), Expected Effects of Climatic Change on Marine Coastal Ecosystems. Springer Netherlands, Dordrecht, pp. 133–138. https://doi.org/10.1007/978-94-009-2003-3_17.

Appendix A – Bathymetrical maps of the Groningerwad

This Appendix contains in images the division of the Groningerwad area between the different basins for the six available bathymetrical maps. The contour lines of these maps follow the below colour scheme.

Figure 29 Colour scheme of the contour lines of the bathymetrical maps

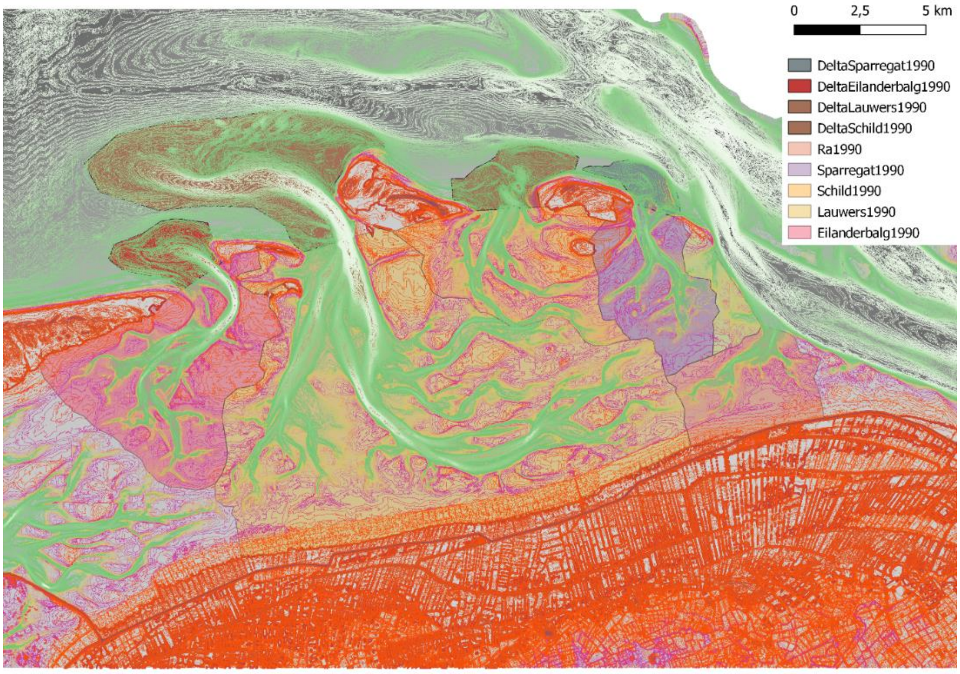

Figure 30 Basin division 1990

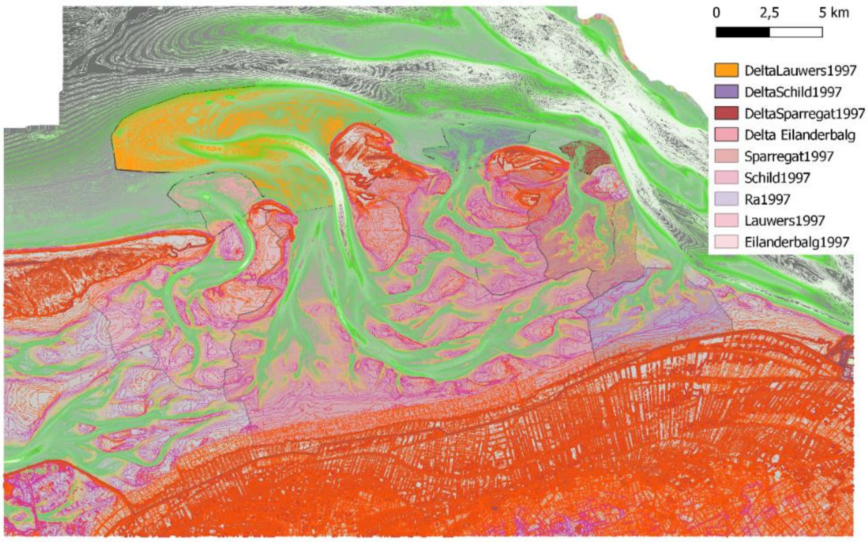

Figure 31 Basin division 1997

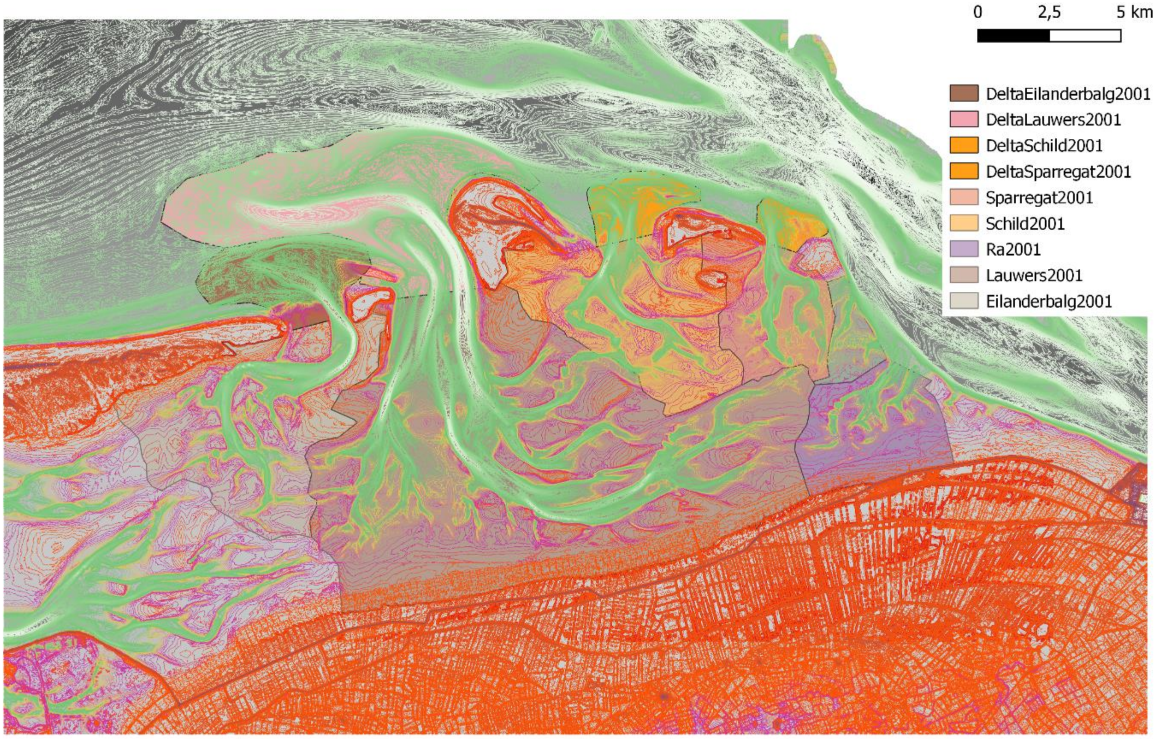

Figure 32 Basin division 2001

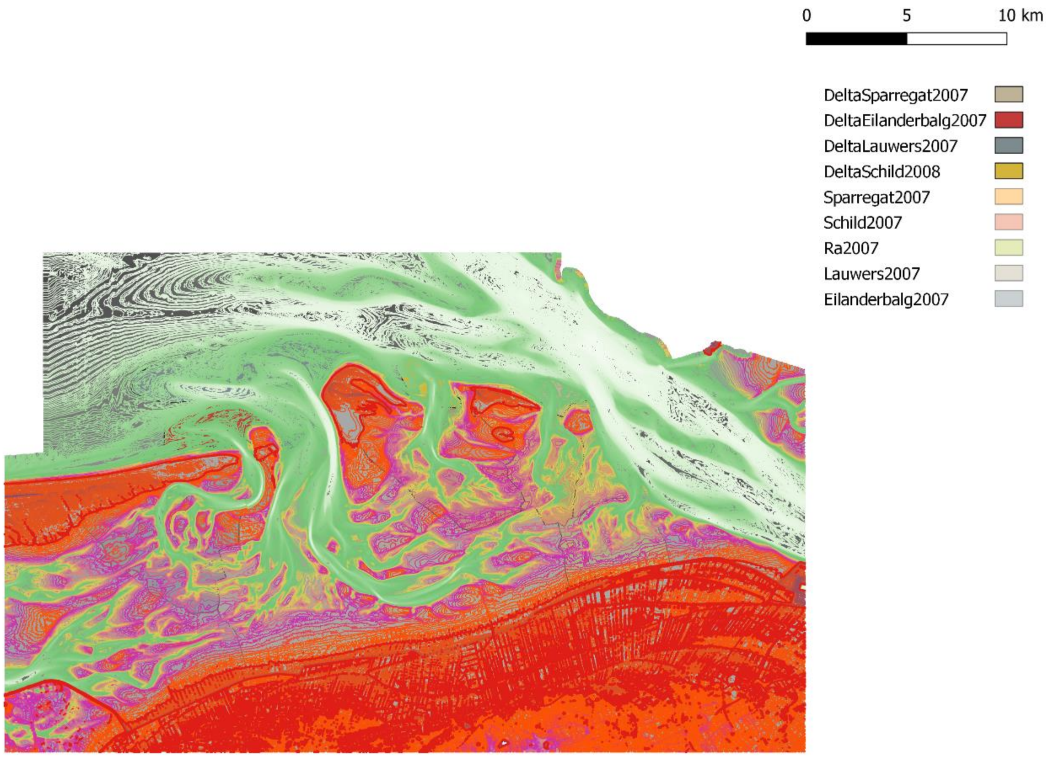

Figure 33 Basin division 2007

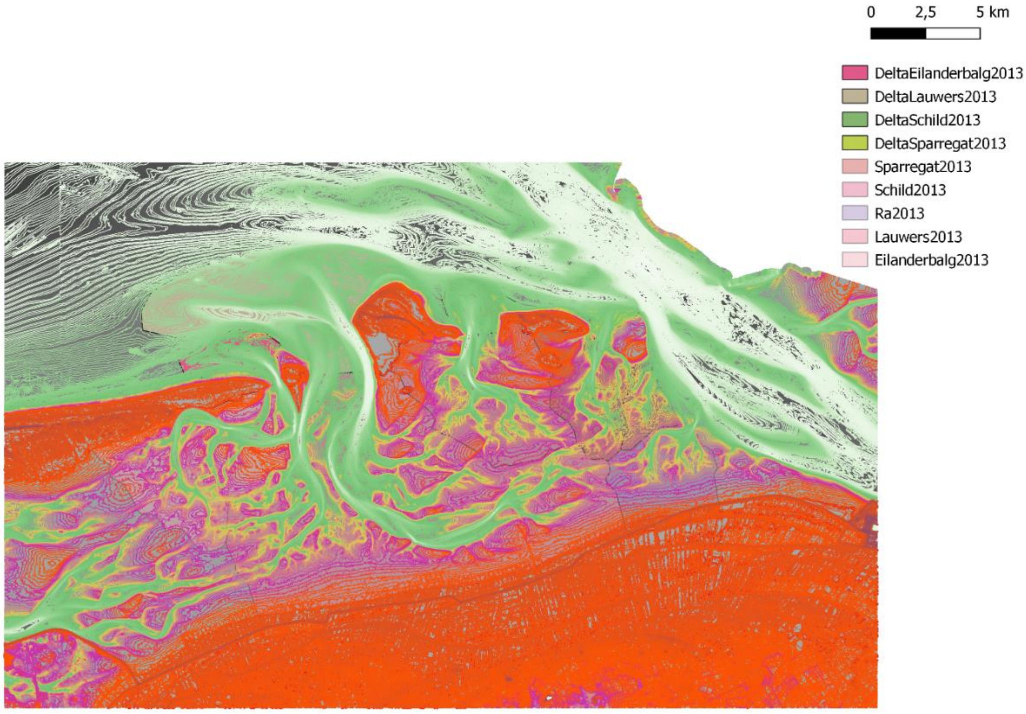

Figure 34 Basin division 2013

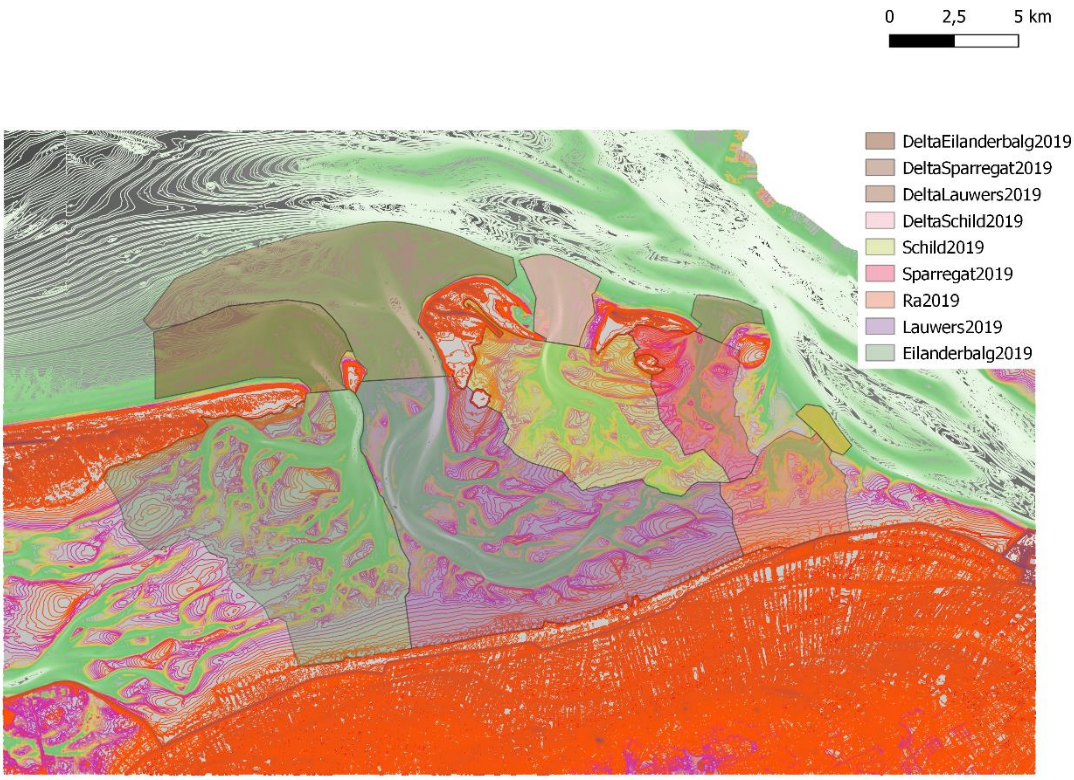

Figure 35 Basin division 2019

Appendix B- Area and volume of the basins

The following table contains the values of the area and volume determined, based on the bathymetry and procedures outlined in chapter 2 for each of the basins of the Groningerwad for each of the bathymetrical maps.

	1990	1997	2001	2007	2013	2019	Average
Eilanderbalg							
Intertidal							
Area [m²]	34818800	34516800	33224800	31619600	32192800	58412400	37464200
Volume [m³]	38201624	38650896	38293136	33499404	32705650	58554028	39984124
Channel							
Area [m²]	7718400	7105200	7582800	8162000	8292000	15356800	9036200
Volume [m³]	19888396	19274652	18578932	19328432	19048644	36150110	22044862
Delta							
Area [m²]	7113200	8102800	13809600	9917600	7963600	21442800	11391600
Volume [m³]	36884607	46678972	73264206	50196205	33845145	52578655	48907965
Lauwers							
Intertidal							
Area [m²]	103439200	94332400	96636000	89894800	88403200	64396400	89517000
Volume [m³]	110569710	98103896	103725704	94770660	94157790	71091864	95403260
Channel							
Area [m²]	39044000	37996800	34771200	34916000	33218000	23121600	33844600
Volume [m³]	114109020	102555490	94302480	91159400	88275410	64695976	92516296
Delta							
Area [m²]	35575600	47258400	41264400	36761200	44126400	41054800	41006800
Volume [m³]	253908674	327083512	267694095	242181659	287147348	296862481	279146295
Schild							
Intertidal							
Area [m²]	22561600	24066000	25791200	28940400	29784000	30942400	27014267
Volume [m³]	22763340	24643570	28219170	30447562	31048856	31257364	28063310
Channel							
Area [m²]	4694000	4842800	5209600	5746000	5397600	6361600	5375267
Volume [m³]	6300813	7760813	9295152	11176559	12318458	13436347	10048023
Delta							
Area [m²]	7959600	7568000	6484800	5390400	6753200	7377600	6922267
Volume [m³]	27633606	25885767	23201389	12671816	23750369	31207001	24058325
Sparregat							
Intertidal							
Area [m²]	17258800	14901200	13467200	14591600	14827600	14123600	14861667
Volume [m³]	15432662	13661792	11498878	12074152	12741746	12394583	12967303
Channel							
Area [m²]	2884800	3185200	3192000	3720800	2490400	1819200	2882067
Volume [m³]	4423033	3637105	4654520	4007538	3210550	2252317	3697511
Delta							
Area [m²]	3698000	2433600	3178400	3753200	3183200	3151600	3233000
Volume [m³]	9465461	7337933	10825323	11966524	10188805	8452248	9706049
Ra							
Intertidal							
Area [m²]	15342000	17769600	16004400	15632000	14800800	14306400	15642533
Volume [m³]	15449102	18028334	15985548	15277230	14303802	13666630	15451775
Channel							
Area [m²]	1910000	1952000	1920000	1492000	1681600	1900000	1809267
Volume [m³]	1890849	1946708	1810792	1520238	1579580	1993349	1790252

Appendix C – Hypsometry per basin

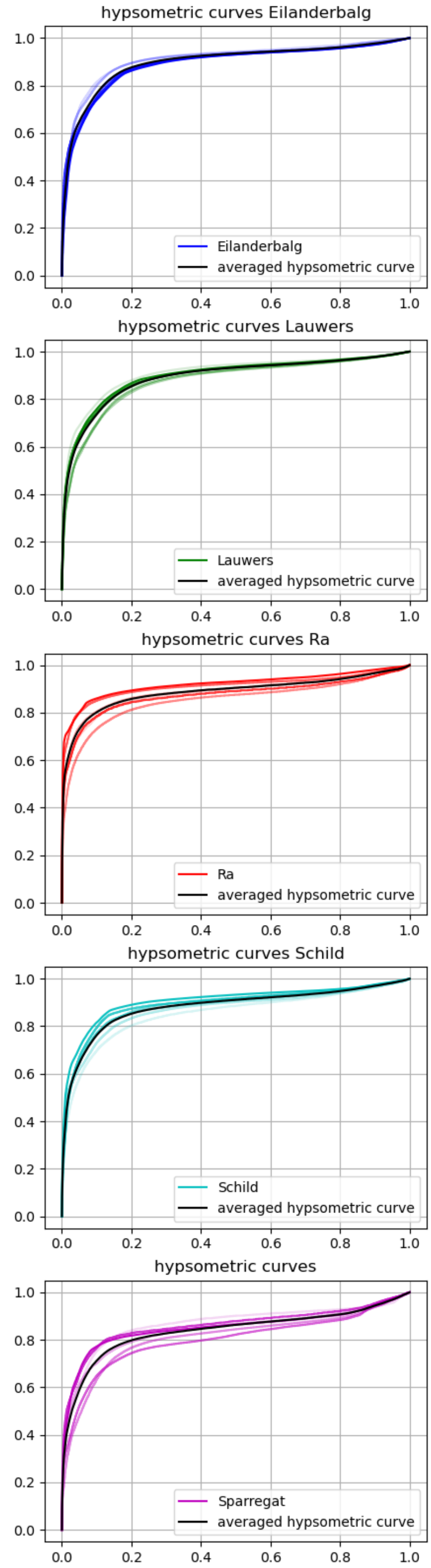

Figure 36 Hypsometric curves normalized both in area and depth.

The hypsometric curves presented here have also been presented in chapter two, but here the graphs are separately depicted per basin. These hypsometric curves are produced by normalising both area and height. Area is normalised to its total area and the height is normalised to the depth up to the 95 percentile, therewith discounting the deepest 5%. This aims to limit the effects of possible measurement error and/or local extremely unusual depths for instance due to local scour holes overly effecting the results. The depth above the value of the 95 percentile is also disregarded in these curves.

These normalised hypsometric curves are used to determine which basin is closest to its equilibrium position. Due to both the normalisation procedure in both area and depth actual volume information is filtered out. However, the assumption is made that as a basin moves to its equilibrium position, not only its volume changes, but also the distribution of said volume across the basin area. Figure 10 of Huisman et al. (2022) shows how a tidal basin fills in. As also mentioned in Huisman et al. (2022) a basin subject to accelerating sea level rise develops in reverse order. But, in the present situation, which is relevant for the determination of which basin is closest to equilibrium, accelerating sea level rise is not relevant. The basin development as described by this image shows that as a basin develops the distribution of volume also changes.

This information, that the distribution of volume is described by the relation of depth and area, is retained even after the normalisation procedure. And thus, these hypsometric curves give an indication of each a basin its proximity to its equilibrium position. If the hypsometric curves, corresponding to the different years for which measurements are available, lie close together the basin is assumed to be closer to its equilibrium position than if the different curves are more divergent.

Consequently, it can be concluded from these graphs that the Eilanderbalg and Lauwers are closest to equilibrium. The Sparregat and Ra basin appear to be furthest from equilibrium whilst the Schild basin is somewhere in between. To further quantify the 'relative' proximity to equilibrium the deviation between the curves and the average curve is determined for every basin.

All curves are interpolated to contain 37870 datapoints. Then the average curve is constructed by averaging across the six curves for every datapoint. The deviation of a curve with the average then follows from subtracting the curve and the average, which is possible as due to the interpolation procedure both curves have the same number of datapoints. The deviation of every curve with respect to its average is shown in the table. Based on the summed total of these deviation the Eilanderbalg basin is closest to equilibrium. Followed by the Lauwers, Schild, Ra and Sparregat.

Basin	Eilanderbalg	Lauwers	Schild	Sparregat	Ra
1990	552	721	1107	1099	238
1997	398	633	504	175	96
2001	263	492	297	1057	1384
2007	221	104	104	1432	833
2013	205	102	412	880	538
2019	412	277	975	524	1209
Sum	2049	2328	3399	5166	4298

Appendix D – Horizontal exchange coefficients

The horizontal exchange coefficients govern the exchange rate between the different elements within a basin. These exchange coefficients (δ) depend on the sediment characteristics and the geometry of the basin. The formulas involved were presented in chapter 3.

Geometry and results

The following table show the geometry and corresponding dispersion coefficient and horizontal exchange coefficients for each basin. The subscripts 'fc', 'cd' and 'do' denote 'flat-channel', 'channel-delta' and 'delta-outside' respectively with 'c' and 'f' denoting the 'coarse' and 'fine' fractions.

input			(intermediate result)		output	
Eilanderbalg						
l_{fc}	1000	m	D_{fc_c}	7,666667	δ_{fc_c}	740,6
l_{cd}	7500	m	D_{fc_f}	2,30E+02	δ_{fc_f}	2,22E+04
l_{wl}	84000	m				
l_{inlet}	1600	m	D_{cd_c}	24	δ_{cd_c}	1,84E+01
$h_{avg\ inlet}$	-3,6	m NAP	D_{cd_f}	7,20E+02	δ_{cd_f}	5,53E+02
$l_{contour\ d}$	11500	m				
$h_{avg\ delta}$	-7	m NAP	D_{do_c}	46,66667	δ_{do_c}	75,13333
l_{od}	50000	m	D_{do_f}	1,40E+03	δ_{do_f}	2,25E+03
Lauwers						
l_{fc}	1500	m	D_{fc_c}	7,666667	δ_{fc_c}	505,4889
l_{cd}	12000	m	D_{fc_f}	2,30E+02	δ_{fc_f}	1,52E+04
l_{wl}	86000	m				
l_{inlet}	3500	m	D_{cd_c}	24,66667	δ_{cd_c}	2,66E+01
$h_{avg\ inlet}$	-3,7	m NAP	D_{cd_f}	7,40E+02	δ_{cd_f}	7,99E+02
$l_{contour\ d}$	17000	m				
$h_{avg\ delta}$	-9	m NAP	D_{do_c}	60	δ_{do_c}	183,6
l_{od}	50000	m	D_{do_f}	1,80E+03	δ_{do_f}	5,51E+03
Schild						
l_{fc}	1250	m	D_{fc_c}	7,666667	δ_{fc_c}	246,8667
l_{cd}	4500	m	D_{fc_f}	2,30E+02	δ_{fc_f}	7,41E+03
l_{wl}	35000	m				
l_{inlet}	1400	m	D_{cd_c}	29,33333	δ_{cd_c}	4,02E+01
$h_{avg\ inlet}$	-4,4	m NAP	D_{cd_f}	8,80E+02	δ_{cd_f}	1,20E+03
$l_{contour\ d}$	5000	m				
$h_{avg\ delta}$	-6	m NAP	D_{do_c}	40	δ_{do_c}	24
l_{od}	50000	m	D_{do_f}	1,20E+03	δ_{do_f}	7,20E+02
Sparregat						
l_{fc}	900	m	D_{fc_c}	7,666667	δ_{fc_c}	111,7366
l_{cd}	3000	m	D_{fc_f}	2,30E+02	δ_{fc_f}	3,35E+03
l_{wl}	11406	m				
l_{inlet}	1000	m	D_{cd_c}	13,33333	δ_{cd_c}	8,89E+00
$h_{avg\ inlet}$	-2	m NAP	D_{cd_f}	4,00E+02	δ_{cd_f}	2,67E+02
$l_{contour\ d}$	4000	m				
$h_{avg\ delta}$	-8	m NAP	D_{do_c}	53,33333	δ_{do_c}	34,13333
l_{od}	50000	m	D_{do_f}	1,60E+03	δ_{do_f}	1,02E+03
Ra						
l_{fc}	750	m	D_{fc_c}	7,666667	δ_{fc_c}	188,0889
l_{cd}	2500	m	D_{fc_f}	2,30E+02	δ_{fc_f}	5,64E+03
l_{wl}	16000	m				
l_{inlet}	750	m	D_{cd_c}	21,33333	δ_{cd_c}	2,05E+01
$h_{avg\ inlet}$	-3,2	m NAP	D_{cd_f}	6,40E+02	δ_{cd_f}	6,14E+02
$l_{contour\ d}$	3500	m				
$h_{avg\ delta}$	-6	m NAP	D_{do_c}	40	δ_{do_c}	16,8
l_{od}	50000	m	D_{do_f}	1,20E+03	δ_{do_f}	5,04E+02

Appendix E – Relation between volume and prism for the intertidal flat, channel and delta.

The ASMITA model relies on equilibrium relations relating volume to the tidal prism. The tidal prism is the water volume which enters, or leaves, a tidal basin every tidal cycle. The exact formulation of these relations is presented in chapter 3. The following graphs show the relation between the tidal prism and the volume of the different elements. Presented in three graphs with a linear scale and three graphs with a log scale along the x-axis.